Sequential and Decentralized Estimation of Linear-Regression Parameters in Wireless Sensor Networks

YASIN YILMAZ
University of Michigan
Ann Arbor, MI, USA

GEORGE V. MOUSTAKIDES
University of Patras
Rio, Greece

XIAODONG WANG
Columbia University
New York, NY, USA

Sequential estimation of a vector of linear-regression coefficients is considered under both centralized and decentralized setups. In sequential estimation, the number of observations used for estimation is determined by the observed samples and hence is random, as opposed to fixed-sample-size estimation. Specifically, after receiving a new sample, if a target accuracy level is reached, we stop and estimate using the samples collected so far; otherwise we continue to receive another sample. It is known that finding an optimum sequential estimator, which minimizes the average observation number for a given target accuracy level, is an intractable problem with a general stopping rule that depends on the complete observation history. By properly restricting the search space to stopping rules that depend on a specific subset of the complete observation history, we derive the optimum sequential estimator in the centralized case via optimal stopping theory. However, finding the optimum stopping rule in this case requires numerical computations that quadratically scale with the number of parameters to be estimated. For the decentralized setup with stringent energy constraints, under an alternative problem formulation that is conditional on the observed regressors, we first derive a simple optimum scheme with a well-defined one-dimensional stopping rule regardless of the number of parameters. Then, following this simple optimum scheme, we propose a decentralized sequential estimator whose computational complexity and energy consumption scale linearly with the number of parameters. Specifically, in the proposed decentralized scheme a close-to-optimum average stopping-time performance is achieved by infrequently transmitting a single pulse with very short duration.

Manuscript received September 8, 2014; revised March 2, 2015; released for publication August 3, 2015.

DOI. No. 10.1109/TAES.2015.140665.

Refereeing of this contribution was handled by S. Marano.

Authors' addresses: Y. Yılmaz, Department of Electrical Engineering and Computer Science, University of Michigan, Ann Arbor, MI 48109, USA, E-mail: (yasiny@umich.edu); G. V. Moustakides, Department of Electrical and Computer Engineering, University of Patras, Rio 26500, Greece, E-mail: (moustaki@upatras.gr); X. Wang, Department of Electrical Engineering, Columbia University, New York, NY 10027, USA, E-mail: (wangx@ee.columbia.edu).

I. INTRODUCTION

In this paper, we are interested in sequentially estimating a vector of parameters (i.e., regression coefficients) $X \in \mathbb{R}^n$ at a random stopping time $\mathcal{T}$ in the linear (regression) model

$$y_t = H_t' X + w_t, \quad t \in \mathbb{N}, \tag{1}$$

where $y_t \in \mathbb{R}$ is the observed sample, $H_t \in \mathbb{R}^n$ is the vector of regressors, $w_t \in \mathbb{R}$ is the additive noise, and the prime symbol denotes the transpose. We consider the general case in which H_t is random and observed at time t, which covers the deterministic H_t case as a special case. This linear model is commonly used in many applications. For example, in system identification, X is the unknown system coefficients, H_t is the (random) input applied to the system, and y_t is the output at time t. Another example is the estimation of wireless channel coefficients, in which X is the unknown channel coefficients, H_t is the transmitted (random) pilot signal, y_t is the received signal, and w_t is the additive channel noise.

Energy constraints are inherent to wireless sensor networks [1]. Since data transmission is the primary source of energy consumption, it is essential to keep transmission rates low in wireless sensor networks, resulting in a decentralized setup. Decentralized parameter estimation is a fundamental task performed in wireless sensor networks [2–13]. In sequential estimation, the objective is to minimize the (average) number of observations for a given target accuracy level [14]. To that end, a sequential estimator $(\mathcal{T}, \hat{X}_{\mathcal{T}})$—as opposed to a traditional fixed-sample-size estimator—is equipped with a stopping rule which determines an appropriate time $\mathcal{T}$ to stop taking new observations based on the observation history. Hence the stopping time $\mathcal{T}$ (i.e., the number of observations used in estimation) is a random variable. Endowed with a stopping mechanism, a sequential estimator saves not only time but also energy, both of which are critical resources. In particular, it avoids unnecessary data processing and transmission.

Decentralized parameter estimation has been mainly studied under three different network topologies. In the first one, sensors communicate to a fusion center (FC) that performs estimation based on the received information, e.g., [3–8]. Another commonly studied topology is called an ad hoc network, in which there is no designated FC; sensors first compute their local estimators (sensing phase) and then communicate them through the network to reach a consensus (communication phase), e.g., [2, 9–12]. Decentralized estimation under both network topologies is reviewed in [13]. Recently, a new class of consensus-based algorithms, in which sensing and

communication phases occur at the same time step, has been proposed for decentralized detection [15–17]. Many existing works consider parameter estimation in linear models—e.g., [2, 3, 5–7, 10]—whereas in [4, 8, 9, 11–13] a general nonlinear signal model is assumed. The majority of existing works on decentralized estimation—e.g., [2–10, 13]—study fixed-sample-size estimation. There are a few works, such as [12, 18, 19], that consider sequential decentralized parameter estimation, as opposed to the significant volume of literature that considers sequential decentralized detection, e.g., [15, 20–26]. Nevertheless, [12] assumes that sensors transmit real numbers, and [18] focuses on continuous-time observations, which can be seen as practical limitations.

In decentralized detection [22, 23] and estimation [19], level-triggered sampling—an adaptive sampling technique which infrequently transmits a few bits, e.g., one bit, from sensors to the FC—has been used to achieve low-rate transmission. It has been also shown that the decentralized schemes based on level-triggered sampling significantly outperform their counterparts based on conventional uniform sampling in terms of average stopping time. We here propose a novel form of level-triggered sampling that infrequently transmits a single pulse from sensors to the FC and at the same time achieves close-to-optimum average stopping-time performance.

The stopping capability of sequential estimators comes at the cost of sophisticated analysis. In most cases, it is not possible with discrete-time observations to find an optimum sequential estimator that attains the sequential Cramér–Rao lower bound (CRLB) if the stopping time $\mathcal{T}$ is adapted to the complete observation history [27]. Alternatively, [28] and more recently [18, 19] considered stopping times that are adapted to a specific subset of the complete observation history, namely the regressors $\{H_t\}$ in (1). This idea of using a restricted stopping time first appeared in [28] with no optimality result. In [18], with continuous-time observations, a sequential estimator with a restricted stopping time that solely depends on $\{H_t\}$ was shown to achieve the sequential version of the CRLB for scalar parameter estimation. In [19], for scalar parameter estimation with discrete-time observations, a similar sequential estimator was shown to achieve the conditional sequential CRLB for the same restricted class of stopping times.

In this paper, with discrete-time observations and considering the restricted class of stopping times that solely depend on $\{H_t\}$, we find the optimum sequential estimators that minimize the average observation number for a given target accuracy level, under two different formulations of the vector parameter-estimation problem. Following the common practice in sequential analysis, we first minimize the average stopping time subject to a constraint on the estimation accuracy, which is a function of the estimator covariance. The optimum solution to this classical problem proves intractable for even a moderate number of unknown parameters; hence, it is not a convenient model for decentralized estimation. Therefore, we next follow an alternative approach and formulate the problem conditioned on the observed $\{H_t\}$ values, which yields a tractable optimum solution for any number of parameters.

Moreover, from the optimum conditional sequential estimator of the alternative approach, we develop a computation- and energy-efficient decentralized scheme based on level-triggered sampling for sequential estimation of vector parameters. We should note here that the proposed vector parameter estimator is by no means a straightforward extension of the scalar parameter estimators in [18, 19, 28]. Firstly, straightforward application of level-triggered sampling to the vector case yields a computational complexity and energy consumption that scale quadratically with the number of unknown parameters. We propose a linearly scaling method, which is analytically justified and numerically shown to perform close to the optimum average stopping-time performance. Secondly, data transmission and thus energy consumption increase with the number of parameters, which may easily become prohibitive for a sensor with limited battery [29]. We address this energy-efficiency issue by infrequently transmitting a single pulse with very short duration, which encodes, in time, the overshoot in level-triggered sampling, thus achieving close-to-optimum performance.

The remainder of the paper is organized as follows. In Section II, we provide background information on linear parameter estimation. Then in Section III, we derive the optimum sequential estimators under the conventional unconditional and alternative conditional problem formulations. In Section IV, using the tractable solution of the conditional formulation as a model, we propose a computation- and energy-efficient decentralized sequential estimator based on level-triggered sampling. Finally, the paper is concluded in Section V. We represent scalars with lowercase letters, vectors with uppercase letters, and matrices with uppercase bold letters.

II. BACKGROUND

In (1), at each time t we observe the sample y_t and the vector H_t, and thus $\{(y_p, H_p)\}_{p=1}^{t}$ are available. We assume that $\{w_t\}$ are independent and identically distributed (i.i.d.) with $\mathsf{E}[w_t] = 0$ and $\mathrm{Var}(w_t) = \sigma^2$. The least-squares (LS) estimator minimizes the sum of squared errors, i.e.,

$$\hat{\mathrm{X}}_t = \arg\min_{X} \sum_{p=1}^{t} \left(y_p - H_p' X\right)^2, \tag{2}$$

and is given by

$$\hat{\mathrm{X}}_t = \left(\sum_{p=1}^{t} H_p H_p'\right)^{-1} \sum_{p=1}^{t} H_p y_p = \left(\boldsymbol{H}_t' \boldsymbol{H}_t\right)^{-1} \boldsymbol{H}_t' Y_t, \tag{3}$$

where $\boldsymbol{H}_t = [\, H_1 \cdots H_t \,]'$ and $Y_t = [\, y_1 \cdots y_t \,]'$. Note that spatial diversity (i.e., a vector of observations and a

regressor matrix at time t) can be easily incorporated in (1) in the same way we deal with temporal diversity. Specifically, in (2) and (3) we would also sum over the spatial dimensions.

Under the Gaussian noise $w_t \sim \mathcal{N}(0, \sigma^2)$, the LS estimator coincides with the minimum-variance unbiased estimator and achieves the CRLB, i.e., $\mathrm{Cov}(\hat{\mathrm{X}}_t|\boldsymbol{H}_t) = \mathrm{CRLB}_t$. To compute the CRLB, given X and $\boldsymbol{H}_t$, we first write the log-likelihood of the vector Y_t as

$$\begin{aligned} L_t &= \log f\left(Y_t|X, \boldsymbol{H}_t\right) \\ &= -\sum_{p=1}^{t} \frac{\left(y_p - H_p' X\right)^2}{2\sigma^2} - \frac{t}{2}\log\left(2\pi\sigma^2\right). \end{aligned} \tag{4}$$

Then, we have

$$\mathrm{CRLB}_t = \left(\mathsf{E}\left[-\frac{\partial^2}{\partial X^2} L_t|\boldsymbol{H}_t\right]\right)^{-1} = \sigma^2 \boldsymbol{U}_t^{-1}, \tag{5}$$

where

$$\mathsf{E}\left[-\frac{\partial^2}{\partial X^2} L_t|\boldsymbol{H}_t\right]$$

is the Fisher information matrix and $\boldsymbol{U}_t \triangleq \boldsymbol{H}_t'\boldsymbol{H}_t$ is a nonsingular matrix. Since $\mathsf{E}[Y_t|\boldsymbol{H}_t] = \boldsymbol{H}_t X$ and $\mathrm{Cov}(Y_t|\boldsymbol{H}_t) = \sigma^2\boldsymbol{I}$, from (3) we have $\mathsf{E}[\hat{\mathrm{X}}_t|\boldsymbol{H}_t] = X$ and $\mathrm{Cov}(\hat{\mathrm{X}}_t|\boldsymbol{H}_t) = \sigma^2\boldsymbol{U}_t^{-1}$; and thus, from (5), $\mathrm{Cov}(\hat{\mathrm{X}}_t|\boldsymbol{H}_t) = \mathrm{CRLB}_t$. Note that the maximum-likelihood estimator, which maximizes (4), coincides with the LS estimator in (3).

In general, the LS estimator is the best linear unbiased estimator. In other words, any linear unbiased estimator of the form $\boldsymbol{A}_t Y_t$ with $\boldsymbol{A}_t \in \mathbb{R}^{n\times t}$, where $\mathsf{E}[\boldsymbol{A}_t Y_t|\boldsymbol{H}_t] = X$, has a covariance no smaller than that of the LS estimator in (3)—i.e., $\mathrm{Cov}(\boldsymbol{A}_t Y_t|\boldsymbol{H}_t) \geq \sigma^2\boldsymbol{U}_t^{-1}$ in the positive-semidefinite sense. To see this result we write $\boldsymbol{A}_t = (\boldsymbol{H}_t'\boldsymbol{H}_t)^{-1}\boldsymbol{H}_t' + \boldsymbol{B}_t$ for some $\boldsymbol{B}_t \in \mathbb{R}^{n\times t}$, and then $\mathrm{Cov}(\boldsymbol{A}_t Y_t|\boldsymbol{H}_t) = \sigma^2\boldsymbol{U}_t^{-1} + \sigma^2\boldsymbol{B}_t\boldsymbol{B}_t'$, where $\boldsymbol{B}_t\boldsymbol{B}_t'$ is a positive-semidefinite matrix.

The recursive least-squares algorithm enables us to compute $\hat{\mathrm{X}}_t$ in a recursive way as follows:

$$\hat{\mathrm{X}}_t = \hat{\mathrm{X}}_{t-1} + K_t\left(y_t - H_t'\hat{\mathrm{X}}_{t-1}\right), \tag{6}$$

where

$$K_t = \frac{\boldsymbol{P}_{t-1}H_t}{1 + H_t'\boldsymbol{P}_{t-1}H_t} \in \mathbb{R}^n$$

is a gain vector and $\boldsymbol{P}_t = \boldsymbol{P}_{t-1} - K_t H_t'\boldsymbol{P}_{t-1} = \boldsymbol{U}_t^{-1}$. In applying the recursive least-squares algorithm we first initialize $\hat{\mathrm{X}}_0 = 0$ and $\boldsymbol{P}_0 = \delta^{-1}\boldsymbol{I}$—where 0 represents a zero vector and δ is a small number—and then at each time t we compute K_t, $\hat{\mathrm{X}}_t$, and $\boldsymbol{P}_t$ as in (6).

III. OPTIMUM SEQUENTIAL ESTIMATION

In this section we aim to find the optimal pair $(\mathrm{T}, \hat{\mathrm{X}}_{\mathrm{T}})$ of stopping time and estimator corresponding to the optimal sequential estimator. The stopping time for a sequential estimator is determined according to a target estimation accuracy. In general, the average stopping time is minimized subject to a constraint on the estimation accuracy, which is a function of the estimator covariance—i.e.,

$$\min_{\mathcal{T}, \hat{X}_{\mathcal{T}}} \mathsf{E}\left[\mathcal{T}\right] \text{ subject to } f\left(\mathrm{Cov}\left(\hat{X}_{\mathcal{T}}\right)\right) \leq c, \tag{7}$$

where $f(\cdot)$ is a function from $\mathbb{R}^{n\times n}$ to $\mathbb{R}$ and $c \in \mathbb{R}$ is the target accuracy level.

The accuracy function f should be a monotonic function of the covariance matrix $\mathrm{Cov}(\hat{X}_{\mathcal{T}})$, which is positive semidefinite, in order to make consistent accuracy assessments—e.g., $f(\mathrm{Cov}(\hat{X}_{\mathcal{T}})) > f(\mathrm{Cov}(\hat{X}_{\mathcal{S}}))$ for $\mathcal{T} < \mathcal{S}$, since $\mathrm{Cov}(\hat{X}_{\mathcal{T}}) \succ \mathrm{Cov}(\hat{X}_{\mathcal{S}})$ in the positive-definite sense. Two popular and easy-to-compute choices are the trace $\mathrm{Tr}(\cdot)$, which corresponds to the mean squared error (MSE), and the Frobenius norm $\|\cdot\|_F$. Before handling the problem in (7), let us explain why we are interested in restricted stopping times that are adapted to a subset of observation history.

Define $\{\mathcal{F}_t\}$ as the filtration that corresponds to the samples $\{y_1, \ldots, y_t\}$, where $\mathcal{F}_t = \sigma\{y_1, \ldots, y_t\}$ is the σ-algebra generated by the samples observed up to time t—i.e., the accumulated history related to the observed samples—and $\mathcal{F}_0$ is the trivial σ-algebra. Similarly, define the filtration $\{\mathcal{H}_t\}$ where $\mathcal{H}_t = \sigma\{H_1, \ldots, H_t\}$ and $\mathcal{H}_0$ is again the trivial σ-algebra. Firstly, the optimal stopping theory for multidimensional observations is intractable. Secondly, it is known that in general, with discrete-time observations, the sequential CRLB for an unrestricted $\{\mathcal{F}_t \cup \mathcal{H}_t\}$-adapted stopping time is not attainable under any noise distribution except for the Bernoulli noise [27]. On the other hand, in the case of continuous-time observations with continuous paths, the sequential CRLB for an unrestricted stopping time is attained by the LS estimator with an $\{\mathcal{H}_t\}$-adapted stopping time, which depends only on $\boldsymbol{H}_{\mathcal{T}}$ [18]. Furthermore, in Lemma 1 we show that with discrete-time observations, the LS estimator with an $\{\mathcal{H}_t\}$-adapted stopping time attains the conditional sequential CRLB for the $\{\mathcal{H}_t\}$-adapted stopping times. Note that the (conditional) sequential CRLB for the $\{\mathcal{H}_t\}$-adapted stopping times is not the same as that for the $\{\mathcal{F}_t \cup \mathcal{H}_t\}$-adapted stopping times. The latter is tighter, since an $\{\mathcal{H}_t\}$-adapted stopping time is also $\{\mathcal{F}_t \cup \mathcal{H}_t\}$-adapted.

LEMMA 1 *With a monotonic accuracy function f and an $\{\mathcal{H}_t\}$-adapted stopping time $\mathcal{T}$, we can write*

$$f\left(\mathrm{Cov}\left(\hat{X}_{\mathcal{T}}|\boldsymbol{H}_{\mathcal{T}}\right)\right) \geq f\left(\sigma^2\boldsymbol{U}_{\mathcal{T}}^{-1}\right) \tag{8}$$

for all unbiased estimators under Gaussian noise and all linear unbiased estimators under non-Gaussian noise, and the LS estimator

$$\hat{\mathrm{X}}_{\mathcal{T}} = \boldsymbol{U}_{\mathcal{T}}^{-1}V_{\mathcal{T}}, \quad \boldsymbol{U}_t = \boldsymbol{H}_t'\boldsymbol{H}_t, \quad V_{\mathcal{T}} \triangleq \boldsymbol{H}_{\mathcal{T}}'Y_{\mathcal{T}} \tag{9}$$

satisfies the inequality in (8) *with equality.*

PROOF Since the LS estimator, with $\mathrm{Cov}(\hat{\mathrm{X}}_t|\boldsymbol{H}_t) = \sigma^2\boldsymbol{U}_t^{-1}$, is the minimum-variance unbiased estimator under Gaussian noise and the best linear unbiased estimator under non-Gaussian noise, we write

$$\begin{aligned} & f\left(\mathrm{Cov}\left(\hat{X}_{\mathcal{T}}|\boldsymbol{H}_{\mathcal{T}}\right)\right) \\ &= f\left(\mathsf{E}\left[\sum_{t=1}^{\infty}\left(\hat{X}_t - X\right)\left(\hat{X}_t - X\right)'\mathbb{1}_{\{t=\mathcal{T}\}}|\boldsymbol{H}_t\right]\right) \\ &= f\left(\sum_{t=1}^{\infty}\mathsf{E}\left[\left(\hat{X}_t - X\right)\left(\hat{X}_t - X\right)'|\boldsymbol{H}_t\right]\mathbb{1}_{\{t=\mathcal{T}\}}\right) \quad (10) \\ &\geq f\left(\sum_{t=1}^{\infty}\sigma^2\boldsymbol{U}_t^{-1}\mathbb{1}_{\{t=\mathcal{T}\}}\right) \quad (11) \\ &= f\left(\sigma^2\boldsymbol{U}_{\mathcal{T}}^{-1}\right) \quad (12) \end{aligned}$$

for all unbiased estimators under Gaussian noise and all linear unbiased estimators under non-Gaussian noise. The indicator function $\mathbb{1}_{\{A\}} = 1$ if A is true, and 0 otherwise. We used the facts that the event $\{\mathcal{T} = t\}$ is $\mathcal{H}_t$-measurable and $\mathsf{E}[(\hat{X}_t - X)(\hat{X}_t - X)'|\boldsymbol{H}_t] = \mathrm{Cov}(\hat{X}_t|\boldsymbol{H}_t) \geq \sigma^2\boldsymbol{U}_t^{-1}$ to write (10) and (11), respectively.

Hence, we here consider $\{\mathcal{H}_t\}$-adapted stopping times, as in [18, 19, 28].

A. The Optimum Sequential Estimator

In this case we assume $\{H_t\}$ are i.i.d. From the constrained optimization problem in (7), using a Lagrange multiplier λ we obtain the following unconstrained optimization problem:

$$\min_{\mathcal{T},\hat{X}_{\mathcal{T}}} \mathsf{E}[\mathcal{T}] + \lambda f\left(\mathrm{Cov}\left(\hat{X}_{\mathcal{T}}\right)\right). \quad (13)$$

For simplicity, we assume a linear accuracy function f so that $f(\mathsf{E}[\cdot]) = \mathsf{E}[f(\cdot)]$—e.g., the trace function $\mathsf{Tr}(\cdot)$. Then our constraint function becomes the sum of the individual variances—i.e., $\mathsf{Tr}(\mathrm{Cov}(\hat{X}_{\mathcal{T}})) = \sum_{i=1}^{n}\mathrm{Var}(\hat{x}_{\mathcal{T}}^i)$. Since $\mathsf{Tr}(\mathrm{Cov}(\hat{X}_{\mathcal{T}})) = \mathsf{Tr}(\mathsf{E}[\mathrm{Cov}(\hat{X}_{\mathcal{T}}|\boldsymbol{H}_{\mathcal{T}})]) = \mathsf{E}[\mathsf{Tr}(\mathrm{Cov}(\hat{X}_{\mathcal{T}}|\boldsymbol{H}_{\mathcal{T}}))]$, we rewrite (13) as

$$\min_{\mathcal{T},\hat{X}_{\mathcal{T}}} \mathsf{E}\left[\mathcal{T} + \lambda\mathsf{Tr}\left(\mathrm{Cov}\left(\hat{X}_{\mathcal{T}}|\boldsymbol{H}_{\mathcal{T}}\right)\right)\right], \quad (14)$$

where the expectation is with respect to $\boldsymbol{H}_{\mathcal{T}}$. From Lemma 1, we see that $\mathsf{Tr}(\mathrm{Cov}(\hat{X}_{\mathcal{T}}|\boldsymbol{H}_{\mathcal{T}}))$ is minimized by the LS estimator, and so is the objective value in (14). Hence, $\hat{\mathrm{X}}_{\mathcal{T}}$ given in (9)—see (6) for recursive computation—is the optimum estimator for the problem in (7).

Since $\mathsf{Tr}(\mathrm{Cov}(\hat{\mathrm{X}}_{\mathcal{T}}|\boldsymbol{H}_{\mathcal{T}})) = \mathsf{Tr}(\sigma^2\boldsymbol{U}_{\mathcal{T}}^{-1})$, to find the optimal stopping time we need to solve the optimization problem

$$\min_{\mathcal{T}} \mathsf{E}\left[\mathcal{T} + \lambda\mathsf{Tr}\left(\sigma^2\boldsymbol{U}_{\mathcal{T}}^{-1}\right)\right], \quad (15)$$

which can be solved by using the optimal stopping theory. Writing (15) in the alternative form

$$\min_{\mathcal{T}} \mathsf{E}\left[\sum_{t=0}^{\mathcal{T}-1} 1 + \lambda\mathsf{Tr}\left(\sigma^2\boldsymbol{U}_{\mathcal{T}}^{-1}\right)\right], \quad (16)$$

we see that the term $\sum_{t=0}^{\mathcal{T}-1} 1$ accounts for the cost of not stopping until time $\mathcal{T}$ and the term $\lambda\mathsf{Tr}(\sigma^2\boldsymbol{U}_{\mathcal{T}}^{-1})$ represents the cost of stopping at time $\mathcal{T}$. Note that $\boldsymbol{U}_t = \boldsymbol{U}_{t-1} + H_t H_t'$, and given $\boldsymbol{U}_{t-1}$, the current state $\boldsymbol{U}_t$ is (conditionally) independent of all previous states; hence $\{\boldsymbol{U}_t\}$ is a Markov process. That is, in (16), the optimal stopping time for a Markov process is sought, which can be found by solving the following Bellman equation:

$$\begin{aligned} & \mathcal{V}(\boldsymbol{U}) \\ &= \min\left\{\underbrace{\lambda\mathsf{Tr}\left(\sigma^2\boldsymbol{U}^{-1}\right)}_{F(\boldsymbol{U})}, \underbrace{1 + \mathsf{E}\left[\mathcal{V}\left(\boldsymbol{U} + H_1 H_1'\right)|\boldsymbol{U}\right]}_{G(\boldsymbol{U})}\right\}, \end{aligned} \quad (17)$$

where the expectation is with respect to H_1 and $\mathcal{V}$ is the optimal cost function. The optimal cost function is obtained by iterating a sequence of functions $\{\mathcal{V}_m\}$ where $\mathcal{V}(\boldsymbol{U}) = \lim_{m\to\infty}\mathcal{V}_m(\boldsymbol{U})$ and

$$\begin{aligned} \mathcal{V}_m(\boldsymbol{U}) = \min\Big\{&\lambda\mathsf{Tr}\left(\sigma^2\boldsymbol{U}^{-1}\right), 1 \\ &+ \mathsf{E}\left[\mathcal{V}_{m-1}\left(\boldsymbol{U} + H_1 H_1'\right)|\boldsymbol{U}\right]\Big\}. \end{aligned}$$

In the optimal stopping theory, dynamic programming is used. Specifically, the original complex optimization problem in (15) is divided into simpler subproblems given by (17). At each time t we are faced with a subproblem consisting of a stopping cost $F(\boldsymbol{U}_t) = \lambda\mathsf{Tr}(\sigma^2\boldsymbol{U}_t^{-1})$ and an expected sampling cost $G(\boldsymbol{U}_t) = 1 + \mathsf{E}[\mathcal{V}(\boldsymbol{U}_{t+1})|\boldsymbol{U}_t]$ to proceed to time $t+1$. Since $\{\boldsymbol{U}_t\}$ is a Markov process and $\{H_t\}$ are i.i.d., (17) is a general equation holding for all t, and thus we drop the time subscript for simplicity. The optimal cost function $\mathcal{V}(\boldsymbol{U}_t)$, selecting the action with minimum cost (i.e., either continue or stop), determines the optimal policy to follow at each time t. That is, we stop the first time the stopping cost is smaller than the average cost of sampling, i.e.,

$$\mathsf{T} = \min\{t \in \mathbb{N} : \mathcal{V}(\boldsymbol{U}_t) = F(\boldsymbol{U}_t)\}.$$

We obviously need to analyze the structure of $\mathcal{V}(\boldsymbol{U}_t)$—i.e., the cost functions $F(\boldsymbol{U}_t)$ and $G(\boldsymbol{U}_t)$—to find the optimal stopping time T. (Refer to [30] for more information on optimal stopping theory.)

Note that $\mathcal{V}$, being a function of the symmetric matrix $\boldsymbol{U} = [u_{ij}] \in \mathbb{R}^{n\times n}$, is a function of $(n^2+n)/2$ variables $\{u_{ij} : i \leq j\}$. Analyzing a multidimensional optimal cost function proves intractable, and thus we will first analyze the special case of scalar-parameter estimation and then provide some numerical results for the two-dimensional vector case, demonstrating how intractable the higher dimensional problems are.

1) *Scalar Case*: For the scalar case, from (17) we have the following one-dimensional optimal cost function:

$$\mathcal{V}(u) = \min\left\{\frac{\lambda\sigma^2}{u}, 1 + \mathsf{E}\left[\mathcal{V}\left(u + h_1^2\right)|u\right]\right\}, \tag{18}$$

where the expectation is with respect to the scalar coefficient h_1. Specifically, at time t the optimal cost function is written as

$$\mathcal{V}(u_t) = \min\left\{\frac{\lambda\sigma^2}{u_t}, 1 + \mathsf{E}\left[\mathcal{V}(u_{t+1})|u_t\right]\right\},$$

where $u_{t+1} = u_t + h_{t+1}^2$. Writing $\mathcal{V}$ as a function of $z_t \triangleq 1/u_t$, we have $\mathcal{V}(z_t) = \min\{\lambda\sigma^2 z_t, 1 + \mathsf{E}[\mathcal{V}(z_{t+1})|z_t]\}$, where $z_{t+1} = z_t/(1 + z_t h_{t+1}^2)$, and thus in general

$$\mathcal{V}(z) = \min\left\{\underbrace{\lambda\sigma^2 z}_{F(z)}, \underbrace{1 + \mathsf{E}\left[\mathcal{V}\left(\frac{z}{1 + zh_1^2}\right)|z\right]}_{G(z)}\right\}. \tag{19}$$

We need to analyze the cost functions $F(z) = \lambda\sigma^2 z$ and

$$G(z) = 1 + \mathsf{E}\left[\mathcal{V}\left(\frac{z}{1 + zh_1^2}\right)|z\right].$$

The former is a line, whereas the latter is, in general, a nonlinear function of z. We have Lemma 2 regarding the structure of $\mathcal{V}(z)$ and $G(z)$. Its proof is given in the Appendix.

LEMMA 2 *The optimal cost $\mathcal{V}$ and the expected sampling cost G, given in* (19)*, are nondecreasing, concave, and bounded functions of z.*

Following Lemma 2, Theorem 1 presents the stopping time for the scalar case of the problem in (7).

THEOREM 1 *The optimal stopping time for the scalar case of the problem in* (7) *with* $\mathsf{Tr}(\cdot)$ *as the accuracy function is given by*

$$\mathsf{T} = \min\left\{t \in \mathbb{N} : u_t \geq \frac{1}{\acute{c}}\right\}, \tag{20}$$

where $\acute{c}$ is selected so that

$$\mathsf{E}\left[\frac{\sigma^2}{u_\mathsf{T}}\right] = c,$$

i.e., the variance of the estimator exactly hits the target accuracy level c (see Algorithm 1).

PROOF The cost functions $F(z)$ and $G(z)$ are continuous functions, as F is linear and G is concave. From (19) we have $\mathcal{V}(0) = \min\{0, 1 + \mathcal{V}(0)\} = 0$, hence $G(0) = 1 + \mathcal{V}(0) = 1$. Then, using Lemma 2, we illustrate $F(z)$ and $G(z)$ in Fig. 1. The optimal cost function $\mathcal{V}(z)$, being the minimum of F and G—see (19)—is also shown in Fig. 1. Note that as t increases, z tends from infinity to zero. Hence, we continue until the stopping cost $F(z_t)$ is lower than the expected sampling cost $G(z_t)$—i.e., until $z_t \leq \acute{c}$. The threshold $\acute{c}(\lambda) = \{z : F(\lambda, z) = G(z)\}$ is determined by the Lagrange multiplier λ, which, from (13), is selected to satisfy the constraint

$$\mathsf{Var}(\hat{x}_\mathsf{T}) = \mathsf{E}\left[\frac{\sigma^2}{u_\mathsf{T}}\right] = c.$$

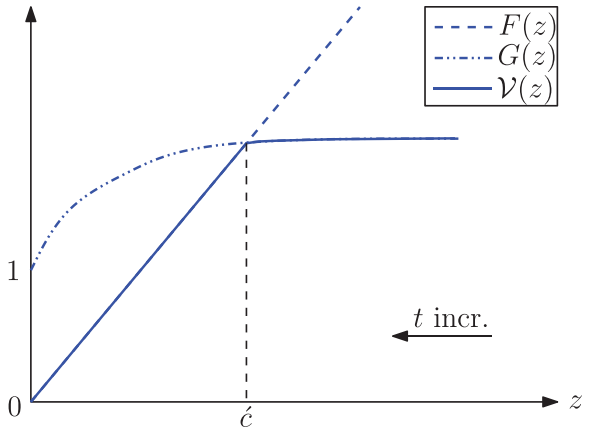

Fig. 1. Structures of optimal cost function $\mathcal{V}(z)$ and cost functions $F(z)$ and $G(z)$.

ALGORITHM 1 The procedure to compute the threshold $\acute{c}$ for given c

1: Select $\acute{c}$
2: Estimate $\boldsymbol{C} = \mathsf{E}\left[\frac{\sigma^2}{u_\mathsf{T}}\right]$ through simulations, where $u_t = \sum_{p=1}^{t} h_p^2$ and $\mathsf{T} = \min\{t \in \mathbb{N} : u_t \geq \frac{1}{\acute{c}}\}$
3: **if** $\boldsymbol{C} = c$ **then**
4: return $\acute{c}$
5: **else**
6: **if** $\boldsymbol{C} > c$ **then**
7: Decrease $\acute{c}$
8: **else**
9: Increase $\acute{c}$
10: **end if**
11: Go to line 2
12: **end if**

In Algorithm 1, we show how to determine the threshold $\acute{c}$.

We see from Theorem 1 that the optimum stopping time in the scalar case is given by a threshold rule on the Fisher information.

2) *Two-Dimensional Case*: We will next show that the multidimensional cases are intractable by providing some numerical results for the two-dimensional case. In the two-dimensional case, we have

$$\mathsf{Tr}\left(\sigma^2 \boldsymbol{U}^{-1}\right) = \sigma^2 \frac{u_{11} + u_{22}}{u_{11}u_{22} - u_{12}^2},$$

where

$$\boldsymbol{U} = \begin{bmatrix} u_{11} & u_{12} \\ u_{12} & u_{22} \end{bmatrix}, \quad H_1 = \begin{bmatrix} h_{1,1} \\ h_{1,2} \end{bmatrix}.$$

Hence, from (17) the optimal cost function is written as

$$\mathcal{V}(u_{11}, u_{12}, u_{22}) = \min\left\{\lambda\sigma^2 \frac{u_{11}+u_{22}}{u_{11}u_{22}-u_{12}^2}, 1 + \mathsf{E}\left[\mathcal{V}\left(u_{11}+h_{1,1}^2, u_{12}+h_{1,1}h_{1,2}, u_{22}+h_{1,2}^2\right)|\boldsymbol{U}\right]\right\}, \tag{21}$$

where the expectation is with respect to $h_{1,1}$ and $h_{1,2}$. Changing variables, we can write $\mathcal{V}$ as a function of $z_{11} \triangleq 1/u_{11}$, $z_{22} \triangleq 1/u_{22}$, and $\rho \triangleq u_{12}/\sqrt{u_{11}u_{22}}$:

$$\mathcal{V}(z_{11}, z_{22}, \rho) = \min\left\{\underbrace{\lambda\sigma^2\frac{z_{11}+z_{22}}{1-\rho^2}}_{F(z_{11},z_{22},\rho)}, \underbrace{1 + \mathsf{E}\left[\mathcal{V}\left(\frac{z_{11}}{1+z_{11}h_{1,1}^2}, \frac{z_{22}}{1+z_{22}h_{1,2}^2}, \frac{\rho+h_{1,1}h_{1,2}\sqrt{z_{11}z_{22}}}{\sqrt{\left(1+z_{11}h_{1,1}^2\right)\left(1+z_{22}h_{1,2}^2\right)}}\right)|z_{11}, z_{22}, \rho\right]}_{G(z_{11},z_{22},\rho)}\right\}, \tag{22}$$

which can be iteratively computed as

$$\mathcal{V}_m(z_{11}, z_{22}, \rho) = \min\left\{\lambda\sigma^2\frac{z_{11}+z_{22}}{1-\rho^2}, 1 + \mathsf{E}\left[\mathcal{V}_{m-1}\left(\frac{z_{11}}{1+z_{11}h_{1,1}^2}, \frac{z_{22}}{1+z_{22}h_{1,2}^2}, \frac{\rho+h_{1,1}h_{1,2}\sqrt{z_{11}z_{22}}}{\sqrt{\left(1+z_{11}h_{1,1}^2\right)\left(1+z_{22}h_{1,2}^2\right)}}\right)|z_{11}, z_{22}, \rho\right]\right\}, \tag{23}$$

where $\lim_{m\to\infty}\mathcal{V}_m = \mathcal{V}$.

Note that ρ is the correlation coefficient, hence we have $\rho \in [-1, 1]$. Following the procedure in Algorithm 2, we numerically compute $\mathcal{V}$ from (23) and find the boundary surface

$$\boldsymbol{S}(\lambda) = \{(z_{11}, z_{22}, \rho) : F(\lambda, z_{11}, z_{22}, \rho) = G(z_{11}, z_{22}, \rho)\}$$

that defines the stopping rule. In Algorithm 2, first the three-dimensional grid ($n_1$dz, $n_2$dz, $n_3$dr) is constructed, where $n_1, n_2 = 0, \ldots,$ Rz/dz and $n_3 = -1/\text{dr}, \ldots, 1/\text{dr}$. Then in lines 4–6 the stopping cost F is computed—see (22)—and in line 7 the first iteration of the optimal cost function $\mathcal{V}_1$ with $\mathcal{V}_0 = 0$ is computed over the grid. In lines 9–28, the optimal cost function $\mathcal{V}$ is computed for each point in the grid by iterating $\mathcal{V}_m$—see (23)—until no significant change occurs between $\mathcal{V}_m$ and $\mathcal{V}_{m+1}$. In each iteration, in lines 13–21 the expectation in (23) with respect to $h_{1,1}$ and $h_{1,2}$ is computed through Monte Carlo calculations. While computing the expectation, since the updated (future) values of (z_{11}, z_{22}, ρ)—i.e, the arguments of $\mathcal{V}_{m-1}$ in (23)—in general may not correspond to a grid point, we average the $\mathcal{V}_{m-1}$ values of eight neighboring grid points with appropriate weights in lines 17–20 to obtain the desired $\mathcal{V}_{m-1}$ value.

The results for $\lambda \in \{0.01, 1, 100\}$, $\sigma^2 = 1$, and $h_{1,1}, h_{1,2} \sim \mathcal{N}(0, 1)$ are shown in Figs. 2 and 3. For $\lambda = 1$, the dome-shaped surface in Fig. 2 separates the stopping region from the continuing region.

Outside the "dome," $\mathcal{V} = G$, and hence we continue. As time progresses, $z_{t,11}$ and $z_{t,22}$ decrease, so we move towards the "dome." Whenever we are inside the "dome" (e.g., at the fifth sample in Fig. 2), we stop, i.e., $\mathcal{V} = F$. We obtain similar dome-shaped surfaces for different λ values. However, the cross sections of the "domes" at specific ρ_t values differ significantly. In particular, we investigate the case of $\rho_t = 0$, where the scaling coefficients $h_{t,1}$ and $h_{t,2}$ are uncorrelated. For small values of λ—e.g., $\lambda = 0.01$—the boundary that separates the stopping and the continuing regions is highly nonlinear, as shown in Fig. 3a. In Figs. 3b, 3c, it is seen that the boundary tends to become more and more linear as λ increases.

Now let us explain the meaning of the λ value. Firstly, note from (22) that F and G are functions of z_{11}, z_{22} for fixed ρ, and the boundary is the solution to $F(\lambda, z_{11}, z_{22}) = G(z_{11}, z_{22})$. When λ is small, the region where $F < G$—i.e., the stopping region—is large, and hence we stop early, as shown in Fig. 3a.[1] Conversely, for large λ the stopping region is small, and hence the stopping time is large (see Fig. 3c). In fact, the Lagrange multiplier λ is selected through simulations following the procedure in Algorithm 3 so that the constraint

$$\mathsf{Tr}\left(\mathsf{E}\left[\sigma^2\boldsymbol{U}_{\mathsf{T}}^{-1}\right]\right) = \mathsf{E}\left[\sigma^2\frac{z_{\mathsf{T},11}+z_{\mathsf{T},22}}{1-\rho_{\mathsf{T}}^2}\right] = c$$

is satisfied. Note that line 2 of Algorithm 3 uses Algorithm 2 to compute the boundary surface $\boldsymbol{S}$.

REMARKS In general, we need to numerically compute the stopping rule—i.e., the hypersurface that separates the stopping and the continuing regions—off-line for a given target accuracy level c. This becomes a quite intractable task, as the dimension n of the vector to be estimated

[1] Note that the axis scales in Fig. 3a are on the order of hundreds, and $z_{t,11}$, $z_{t,22}$ decrease as t increases.

ALGORITHM 2 The procedure to compute the boundary surface $\boldsymbol{S}$ for given λ

Set dz, Rz, dr, Nh, Nz $= \frac{\text{Rz}}{\text{dz}} + 1$, and Nr $= \frac{2}{\text{dr}} + 1$
$z_1 = [0 : \text{dz} : \text{Rz}]$; $z_2 = z_1$; $\rho = [-1 : \text{dr} : 1]$ {all row vectors}
$Z_1 = \mathbf{1}_{\text{Nz}} z_1$; $Z_2 = Z_1'$ {$\mathbf{1}_{\text{Nz}}$: column vector of ones in $\mathbb{R}^{\text{Nz}}$}
for $i = 1 : \text{Nr}$ **do**
  $F(:, :, i) = \lambda \frac{Z_1 + Z_2}{1 - \rho(i)^2}$ {stopping cost over the 3-D grid}
end for
$\mathcal{V} = \min(F, 1)$ {start with $\mathcal{V}_0 = 0$}
dif $= \infty$; Fr $= \|\mathcal{V}\|_{\text{F}}$
while dif $> \delta$Fr {δ: a small threshold} **do**
  for $i = 1 : \text{Nz}^2$ **do**
    $z_{11} = Z_1(i)$; $z_{22} = Z_2(i)$ {linear indexing in matrices}
    for $j = 1 : \text{Nr}$ **do**
      Generate $h_1^{\text{Nh}\times 1}$ and $h_2^{\text{Nh}\times 1}$ {e.g., according to $\mathcal{N}(0, 1)$}
      $Z_{11}' = z_{11}./(1 + z_{11} h_1.^2)$; $Z_{22}' = z_{22}./(1 + z_{22} h_2.^2)$ {dot denotes element-wise operation}
      $\rho' = [\rho(j) + h_1. * h_2 \sqrt{z_{11} z_{22}}]./\sqrt{(1 + z_{11} h_1.^2)(1 + z_{22} h_2.^2)}$ {vector}
      $I_1 = Z_{11}'/\text{dz} + 1$; $I_2 = Z_{22}'/\text{dz} + 1$; $I_3 = (\rho' + 1)/\text{dr} + 1$ {fractional indices}
      $J^{8\times \text{Nh}} =$ linear indices of eight neighbor points using $\lfloor I_n \rfloor$, $\lceil I_n \rceil$, $n = 1, 2, 3$
      $D_n = \lceil I_n \rceil - I_n$; $\bar{D}_n = 1 - D_n$, $n = 1, 2, 3$ {distances to neighbor indices}
      $W^{8\times \text{Nh}} =$ weights for neighbors as eight multiplicative combinations of D_n, $\bar{D}_n$, $n = 1, 2, 3$
      $V^{\text{Nh}\times 1} = \text{diag}(W' \mathcal{V}(J))$ {average the neighbor $\mathcal{V}$ values}
      $G = \text{sum}(V)/\text{Nh}$ {continuing cost}
      $\ell = i + (j - 1)\text{Nz}^2$ {linear index of the point on the 3-D grid}
      $\mathcal{V}'(\ell) = \min(F(\ell), 1 + G)$ {new optimal cost function}
    end for
  end for
  dif $= \|\mathcal{V}' - \mathcal{V}\|_{\text{F}}$; Fr $= \|\mathcal{V}\|_{\text{F}}$
  $\mathcal{V} = \mathcal{V}'$ {update the optimal cost function}
end while
Find the points where transition occurs between regions $\mathcal{V} = F$ and $\mathcal{V} \neq F$, i.e., $\boldsymbol{S}$.

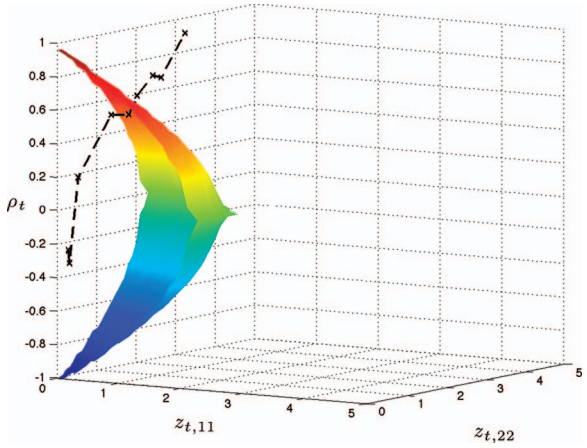

Fig. 2. Surface that defines stopping rule for $\lambda = 1$, $\sigma^2 = 1$, and $h_{1,1}, h_{1,2} \sim \mathcal{N}(0, 1)$ in two-dimensional case. Sample path which stops at fifth sample is also shown.

increases because we find the separating hypersurface in an $(n^2 + n)/2$-dimensional space. Recall from (17) that the optimal cost function $\mathcal{V}$ is a function of the matrix $\boldsymbol{U}$, which has $(n^2 + n)/2$ distinct entries. On the other hand, conditioning the problem formulation in (7) on the observed regressors $\{H_t\}$, we next show that for any n, the optimum stopping rule takes a simple one-dimensional form. We can much more easily decentralize such a tractable optimum solution offered by the conditional formulation than the one given by the cumbersome procedure in Algorithm 2.

B. The Optimum Conditional Sequential Estimator

In the presence of an ancillary statistic whose distribution does not depend on the parameters to be estimated, such as the regressor matrix $\boldsymbol{H}_t$, the conditional covariance $\text{Cov}(\hat{X}_t|\boldsymbol{H}_t)$ can be used to assess the accuracy of the estimator more precisely than the (unconditional) covariance, which is in fact the mean of the former [28, 31]—i.e., $\text{Cov}(\hat{X}_\mathcal{T}) = \text{E}[\text{Cov}(\hat{X}_t|\boldsymbol{H}_t)]$. This is known as the conditionality principle. Motivated by this fact, we propose to reformulate the problem in (7) conditioned on $\boldsymbol{H}_t$:

$$\min_{\mathcal{T}, \hat{X}_\mathcal{T}} \text{E}[\mathcal{T}] \text{ such that } f\left(\text{Cov}\left(\hat{X}_\mathcal{T}|\boldsymbol{H}_\mathcal{T}\right)\right) \leq c. \tag{24}$$

Note that the constraint in (24) is stricter than the one in (7), since it requires that $\hat{X}_\mathcal{T}$ satisfies the target accuracy level for each realization of $\boldsymbol{H}_\mathcal{T}$, whereas in (7) it is sufficient that it satisfies the target accuracy level on average. In other words, in (7), even if $f(\text{Cov}(\hat{X}_\mathcal{T}|\boldsymbol{H}_\mathcal{T})) > c$ for some realizations of $\boldsymbol{H}_\mathcal{T}$, we can still satisfy $f(\text{Cov}(\hat{X}_\mathcal{T})) \leq c$. In fact, we can always have $f(\text{Cov}(\hat{X}_\mathcal{T})) = c$ by using a probabilistic stopping rule such that we sometimes stop above c—i.e., $f(\text{Cov}(\hat{X}_\mathcal{T}|\boldsymbol{H}_\mathcal{T})) > c$—and the rest of the time at or below c—i.e., $f(\text{Cov}(\hat{X}_\mathcal{T}|\boldsymbol{H}_\mathcal{T})) \leq c$. On the other hand, in (24) we always have $f(\text{Cov}(\hat{X}_\mathcal{T}|\boldsymbol{H}_\mathcal{T})) \leq c$, and moreover,

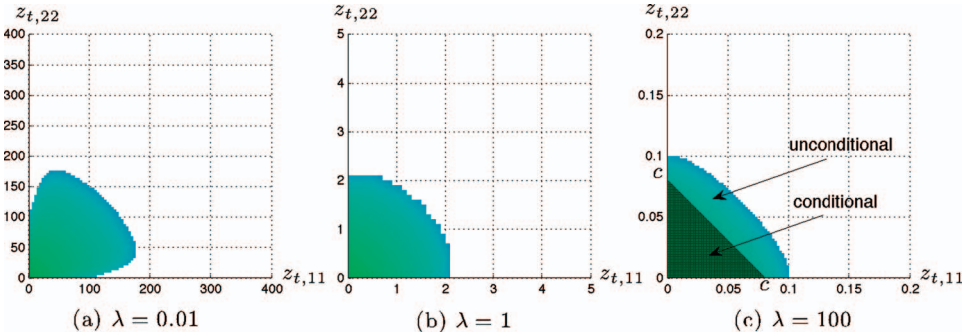

Fig. 3. Stopping regions for $\rho_t = 0$, $\sigma^2 = 1$, and $h_{t,1}, h_{t,2} \sim \mathcal{N}(0, 1) \quad \forall t$ with (a) $\lambda = 0.01$, (b) $\lambda = 1$, (c) $\lambda = 100$. Conditional problem (see Section III-B) is also shown in (c).

ALGORITHM 3 The procedure to compute the boundary surface $\boldsymbol{S}$

1: Select λ
2: Compute $\boldsymbol{S}(\lambda)$ as in Algorithm 2
3: Estimate $\boldsymbol{C} = \mathrm{E}\left[\sigma^2 \frac{z_{\mathsf{T},11}+z_{\mathsf{T},22}}{1-\rho_{\mathsf{T}}^2}\right]$ through simulations, where $z_{t,11} = 1/u_{t,11}$, $z_{t,22} = 1/u_{t,22}$, $\rho_t = u_{t,12}/\sqrt{u_{t,11}u_{t,22}}$, and $\mathsf{T} = \min\{t \in \mathbb{N} : (z_{t,11}, z_{t,22}, \rho_t)\}$ is between $\boldsymbol{S}$ and the origin
4: **if** $\boldsymbol{C} = c$ **then**
5: return $\boldsymbol{S}$
6: **else**
7: **if** $\boldsymbol{C} > c$ **then**
8: Increase λ
9: **else**
10: Decrease λ
11: **end if**
12: Go to line 2
13: **end if**

since we observe discrete-time samples, in general we have $f(\mathrm{Cov}(\hat{X}_{\mathcal{T}}|\boldsymbol{H}_{\mathcal{T}})) < c$ for each realization of $\boldsymbol{H}_{\mathcal{T}}$. Hence, the optimal objective value $\mathrm{E}[\mathcal{T}]$ in (7) will, in general, be smaller than that in (24). Note that on the other hand, if we observed continuous-time processes with continuous paths, we could always have $f(\mathrm{Cov}(\hat{X}_{\mathcal{T}}|\boldsymbol{H}_{\mathcal{T}})) = c$ for each realization of $\boldsymbol{H}_{\mathcal{T}}$, and thus the optimal objective values of (24) and (7) would be the same.

Since minimizing $\mathcal{T}$ also minimizes $\mathrm{E}[\mathcal{T}]$, in (24) we want to find the first time that a member of our class of estimators (i.e., unbiased estimators under Gaussian noise and linear unbiased estimators under non-Gaussian noise) satisfies the constraint $f(\mathrm{Cov}(\hat{X}_{\mathcal{T}}|\boldsymbol{H}_{\mathcal{T}})) \leq c$, as well as the estimator that attains this earliest stopping time. From Lemma 1, it is seen that the LS estimator, given by (9), achieves the best accuracy level $f(\sigma^2\boldsymbol{U}_{\mathcal{T}}^{-1})$ among its competitors at any $\{\mathcal{H}_t\}$-adapted stopping time $\mathcal{T}$. Hence, for the conditional problem, the optimum sequential estimator is composed of the stopping time

$$\mathsf{T} = \min\left\{t \in \mathbb{N} : f\left(\sigma^2\boldsymbol{U}_t^{-1}\right) \leq c\right\} \tag{25}$$

and the LS estimator

$$\hat{\mathrm{X}}_T = \boldsymbol{U}_{\mathsf{T}}^{-1} V_{\mathsf{T}}, \tag{26}$$

which can be computed recursively as in (6). The recursive computation of $\boldsymbol{U}_t^{-1} = \boldsymbol{P}_t$ in the test statistic in (25) is also given in (6). Note that for an accuracy function f such that $f(\sigma^2\boldsymbol{U}_t^{-1}) = \sigma^2 f(\boldsymbol{U}_t^{-1})$—e.g., $\mathrm{Tr}(\cdot)$ and $\|\cdot\|_{\mathrm{F}}$—we can use the stopping time

$$\mathsf{T} = \min\left\{t \in \mathbb{N} : f\left(\boldsymbol{U}_t^{-1}\right) \leq \bar{c}\right\}, \tag{27}$$

where $\bar{c} = c/\sigma^2$ is the relative target accuracy with respect to the noise power. Hence, given $\bar{c}$ we do not need to know the noise variance σ^2 to run the test given by (27). Note that $\boldsymbol{U}_t = \boldsymbol{H}_t'\boldsymbol{H}_t$ is a nondecreasing positive-semidefinite matrix—i.e., $\boldsymbol{U}_t \succcurlyeq \boldsymbol{U}_{t-1} \quad \forall t$ in the positive-semidefinite sense. Thus, from the monotonicity of f, the test statistic $f(\sigma^2\boldsymbol{U}_t^{-1})$ is a nonincreasing scalar function of time. Specifically, for accuracy functions $\mathrm{Tr}(\cdot)$ and $\|\cdot\|_F$ we can show that if the minimum eigenvalue of $\boldsymbol{U}_t$ tends to infinity as $t \to \infty$, then the stopping time is finite, i.e., $T < \infty$.

In the conditional problem, for any n we have a simple stopping rule given in (27), which uses the target accuracy level c/σ^2 as its threshold and hence is known beforehand. For the special case of scalar-parameter estimation, we do not need a function f to assess the accuracy of the estimator, since instead of a covariance matrix we now have a variance σ^2/u_t, where $u_t = \sum_{p=1}^{t} h_p^2$ and h_t is the scaling coefficient in (1). Hence, from (27) the stopping time in the scalar case is given by

$$\mathsf{T} = \min\left\{t \in \mathbb{N} : u_t \geq \frac{1}{\bar{c}}\right\}, \tag{28}$$

where u_t/σ^2 is the Fisher information at time t. That is, we stop the first time the gathered Fisher information exceeds the threshold $1/c$, which is known.

Note that the optimal stopping time in the scalar case of the unconditional problem, given by (20), is of the same form as (28). In both conditional and unconditional problems, the LS estimator

$$\hat{\mathrm{x}}_{\mathsf{T}} = \frac{v_{\mathsf{T}}}{u_{\mathsf{T}}}$$

is the optimal estimator. The fundamental difference between the optimal stopping times in (28) and (20) is that the threshold $\bar{c} = c/\sigma^2$ in the conditional problem is known beforehand, whereas the threshold $\acute{c}$ in the

unconditional problem needs to be determined through off-line simulations following the procedure in Algorithm 1. We also observe that $\bar{c} \leq \acute{c}$, and hence the optimal objective value $\mathsf{E}[\mathsf{T}]$ of the unconditional problem is in general smaller than that of the conditional problem, as noted earlier in this subsection. This is because the upper bound $\sigma^2\acute{c}$ on the conditional variance σ^2/u_T—see (20)—is also an upper bound for the variance $\mathsf{E}[\sigma^2/u_{\mathsf{T}}] = c$, and the threshold $\bar{c}$ is given by $\bar{c} = c/\sigma^2$.

In the two-dimensional case of the conditional problem with the accuracy function $\mathsf{Tr}(\cdot)$, the optimal stopping time is given by

$$\mathsf{T} = \min\left\{t \in \mathbb{N} : \frac{z_{t,11} + z_{t,22}}{1-\rho_t^2} \leq \frac{c}{\sigma^2}\right\},$$

which is a function of $z_{t,11} + z_{t,22}$ for fixed ρ_t. In Fig. 3c, where $\rho_t = 0$ and $\sigma^2 = 1$, the stopping region (respectively average stopping time) of the conditional problem, which is characterized by a line, is shown to be smaller (respectively larger) than that of the unconditional problem due to the same reasoning in the scalar case.

IV. DECENTRALIZED SEQUENTIAL ESTIMATION

In this section, we propose a computation- and energy-efficient decentralized estimator based on the optimum conditional sequential estimator and level-triggered sampling. Consider a network of K distributed sensors and an FC which is responsible for determining the stopping time and computing the estimator. In practice, due to the stringent energy constraints, sensors must infrequently convey low-rate information to the FC, which is the main concern in the design of a decentralized sequential estimator.

As in (1) each sensor k observes

$$y_t^k = \left(H_t^k\right)' X + w_t^k, \tag{29}$$

where $t \in \mathbb{N}$ and $k = 1, \ldots, K$, as well as the regressor vector $H_t^k = [\, h_{t,1}^k \cdots h_{t,n}^k \,]'$ at time t, where $\{w_t^k\}_{k,t}$ are independent and zero mean—i.e., $\mathsf{E}[w_t^k] = 0 \quad \forall k, t$ and $\mathsf{Var}(w_t^k) = \sigma_k^2 \quad \forall t$.[2] Then, similar to (3), the weighted least-squares (WLS) estimator

$$\hat{\mathsf{X}}_t = \arg\min_X \sum_{k=1}^{K}\sum_{p=1}^{t} \frac{\left(y_p^k - \left(H_p^k\right)' X\right)^2}{\sigma_k^2}$$

is given by

$$\hat{\mathsf{X}}_t = \left(\sum_{k=1}^{K}\sum_{p=1}^{t} \frac{H_p^k \left(H_p^k\right)'}{\sigma_k^2}\right)^{-1} \sum_{k=1}^{K}\sum_{p=1}^{t} \frac{H_p^k y_p^k}{\sigma_k^2} = \bar{\boldsymbol{U}}_t^{-1} \bar{V}_t, \tag{30}$$

where $\bar{\boldsymbol{U}}_t^k \triangleq (1/\sigma_k^2)\sum_{p=1}^{t} H_p^k (H_p^k)'$, $\bar{V}_t^k \triangleq (1/\sigma_k^2)\sum_{p=1}^{t} H_p^k y_p^k$, $\bar{\boldsymbol{U}}_t = \sum_{k=1}^{K} \bar{\boldsymbol{U}}_t^k$, and $\bar{V}_t = \sum_{k=1}^{K} \bar{V}_t^k$. As before, it can be shown that the WLS estimator $\hat{\mathsf{X}}_t$ in (30) is the best linear unbiased estimator under the general noise distributions. Moreover, in the Gaussian-noise case, where $w_t^k \sim \mathcal{N}(0, \sigma_k^2) \quad \forall t$ for each k, $\hat{\mathsf{X}}_t$ is also the minimum-variance unbiased estimator.

Following the steps in Section III-B, it is straightforward to show that the optimum sequential estimator for the conditional problem in (24) is given by the stopping time

$$\mathsf{T} = \min\left\{t \in \mathbb{N} : f\left(\bar{\boldsymbol{U}}_t^{-1}\right) \leq c\right\} \tag{31}$$

and the WLS estimator $\hat{\mathsf{X}}_t$—see (30). Note that $(\mathsf{T}, \hat{\mathsf{X}}_{\mathsf{T}})$ is achievable only in the centralized case, where all local observations until time t—i.e., $\{(y_p^k, H_p^k)\}_{k,p}$—are available to the FC.[3] Local processes $\{\bar{\boldsymbol{U}}_t^k\}_{k,t}$ and $\{\bar{V}_t^k\}_{k,t}$ are used to compute the stopping time and estimator as in (31) and (30), respectively. On the other hand, in a decentralized system the FC can compute approximations $\tilde{\boldsymbol{U}}_t^k$ and $\tilde{V}_t^k$ and then use these approximations to compute the stopping time and estimator as in (31) and (30), respectively.

A. Key Approximations in the Decentralized Approach

If each sensor k reports $\bar{\boldsymbol{U}}_t^k \in \mathbb{R}^{n\times n}$ and $\bar{V}_t^k \in \mathbb{R}^n$ to the FC in a straightforward way, then $O(n^2)$ terms need to be transmitted, which may not be practical, especially for large n, in a decentralized setup. Similarly, in the literature the distributed implementation of the Kalman filter—which covers the recursive least-squares algorithm as a special case—through its inverse covariance form, namely the information filter, requires the transmission of an $n \times n$ information matrix and an $n \times 1$ information vector (see, e.g., [32]).

To overcome this problem, considering $\mathsf{Tr}(\cdot)$ as the accuracy function f in (31), we propose to transmit only the n diagonal entries of $\bar{\boldsymbol{U}}_t^k$ for each k, yielding linear complexity $O(n)$. Using the diagonal entries of $\bar{\boldsymbol{U}}_t$ we define the diagonal matrix

$$\boldsymbol{D}_t \triangleq \mathrm{diag}\left(d_{t,1}, \ldots, d_{t,n}\right), \tag{32}$$

where

$$d_{t,i} = \sum_{k=1}^{K}\sum_{p=1}^{t} \frac{\left(h_{p,i}^k\right)^2}{\sigma_k^2},$$

$i = 1, \ldots, n$.

We further define the correlation matrix

$$\boldsymbol{R} = \begin{bmatrix} 1 & r_{12} & \cdots & r_{1n} \\ r_{12} & 1 & \cdots & r_{2n} \\ \vdots & \vdots & \ddots & \vdots \\ r_{1n} & r_{2n} & \cdots & 1 \end{bmatrix}, \tag{33}$$

[2] The subscripts k and t in the set notation denote $k = 1, \ldots, K$ and $t \in \mathbb{N}$.

[3] The subscript p in the set notation denotes $p = 1, \ldots, t$.

where

$$r_{ij} = \frac{\sum_{k=1}^{K} \frac{\mathsf{E}\left[h_{t,i}^k h_{t,j}^k\right]}{\sigma_k^2}}{\sqrt{\sum_{k=1}^{K} \frac{\mathsf{E}\left[\left(h_{t,i}^k\right)^2\right]}{\sigma_k^2} \sum_{k=1}^{K} \frac{\mathsf{E}\left[\left(h_{t,j}^k\right)^2\right]}{\sigma_k^2}}},$$

$i, j = 1, \ldots, n$.

PROPOSITION 1 *For sufficiently large t, we can make the following approximations:*

$$\begin{aligned} \bar{\boldsymbol{U}}_t &\cong \boldsymbol{D}_t^{1/2} \boldsymbol{R} \boldsymbol{D}_t^{1/2} \\ \mathsf{Tr}\left(\bar{\boldsymbol{U}}_t^{-1}\right) &\cong \mathsf{Tr}\left(\boldsymbol{D}_t^{-1} \boldsymbol{R}^{-1}\right). \end{aligned} \tag{34}$$

PROOF The approximations are motivated from the special case where $\mathsf{E}[h_{t,i}^k h_{t,j}^k] = 0 \quad \forall k, i, j = 1, \ldots, n, i \neq j$. In this case, by the law of large numbers, the off-diagonal elements of $\bar{\boldsymbol{U}}_t/t$ vanish for sufficiently large t, and thus we have $\bar{\boldsymbol{U}}_t/t \cong \boldsymbol{D}_t/t$ and $\mathsf{Tr}(\bar{\boldsymbol{U}}_t^{-1}) \cong \mathsf{Tr}(\boldsymbol{D}_t^{-1})$. For the general case, where we might have $\mathsf{E}[h_{t,i}^k h_{t,j}^k] \neq 0$ for some k and $i \neq j$, using the diagonal matrix $\boldsymbol{D}_t$ we write

$$\mathsf{Tr}\left(\bar{\boldsymbol{U}}_t^{-1}\right) = \mathsf{Tr}\left(\left(\boldsymbol{D}_t^{1/2} \underbrace{\boldsymbol{D}_t^{-1/2} \bar{\boldsymbol{U}}_t \boldsymbol{D}_t^{-1/2}}_{\boldsymbol{R}_t} \boldsymbol{D}_t^{1/2}\right)^{-1}\right) \tag{35}$$

$$\begin{aligned} &= \mathsf{Tr}\left(\boldsymbol{D}_t^{-1/2} \boldsymbol{R}_t^{-1} \boldsymbol{D}_t^{-1/2}\right) \\ &= \mathsf{Tr}\left(\boldsymbol{D}_t^{-1} \boldsymbol{R}_t^{-1}\right). \end{aligned} \tag{36}$$

Note that each entry $r_{t,ij}$ of the newly defined matrix $\boldsymbol{R}_t$ is a normalized version of the corresponding entry $\bar{u}_{t,ij}$ of $\bar{\boldsymbol{U}}_t$. Specifically,

$$r_{t,ij} = \frac{\bar{u}_{t,ij}}{\sqrt{d_{t,i} d_{t,j}}} = \frac{\bar{u}_{t,ij}}{\sqrt{\bar{u}_{t,ii} \bar{u}_{t,jj}}},$$

$i, j = 1, \ldots, n$, where the last equality follows from the definition of $d_{t,i}$ in (32). Hence, $\boldsymbol{R}_t$ has the same structure as in (33), with entries

$$r_{t,ij} = \frac{\sum_{k=1}^{K} \sum_{p=1}^{t} \frac{h_{p,i}^k h_{p,j}^k}{\sigma_k^2}}{\sqrt{\sum_{k=1}^{K} \sum_{p=1}^{t} \frac{\left(h_{p,i}^k\right)^2}{\sigma_k^2} \sum_{k=1}^{K} \sum_{p=1}^{t} \frac{\left(h_{p,j}^k\right)^2}{\sigma_k^2}}},$$

$i, j = 1, \ldots, n$. For sufficiently large t, by the law of large numbers

$$r_{t,ij} \cong r_{ij} = \frac{\sum_{k=1}^{K} \frac{\mathsf{E}\left[h_{t,i}^k h_{t,j}^k\right]}{\sigma_k^2}}{\sqrt{\sum_{k=1}^{K} \frac{\mathsf{E}\left[\left(h_{t,i}^k\right)^2\right]}{\sigma_k^2} \sum_{k=1}^{K} \frac{\mathsf{E}\left[\left(h_{t,j}^k\right)^2\right]}{\sigma_k^2}}} \tag{37}$$

and $\boldsymbol{R}_t \cong \boldsymbol{R}$, where $\boldsymbol{R}$ is given in (33). Hence, for sufficiently large t we can make the approximations in (34) using (35) and (36).

Fig. 4 corroborates the accuracy approximation in (34).

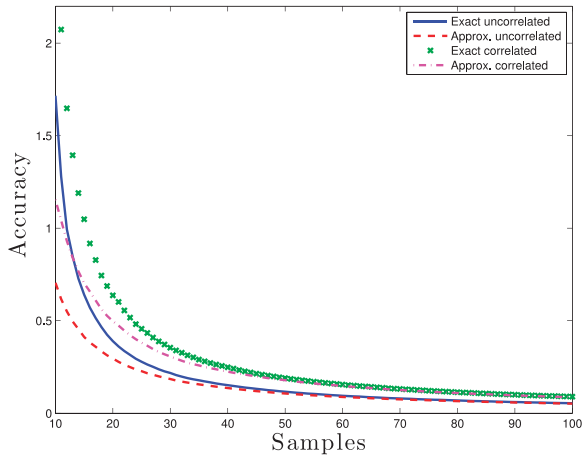

Fig. 4. Accuracy term $\mathsf{Tr}(\bar{\boldsymbol{U}}_t^{-1})$ and its approximation $\mathsf{Tr}(\mathbf{D}_t^{-1}\mathbf{R}^{-1})$ proposed in (34) across time. Both uncorrelated ($r_{ij} = 0 \quad \forall i, j$) and correlated ($r_{ij} = 0.5 \quad \forall i, j$) parameters are investigated.

Then, assuming that the FC knows the correlation matrix $\boldsymbol{R}$—i.e., $\{\mathsf{E}[h_{t,i}^k h_{t,j}^k]\}_{i,j,k}$ and $\{\sigma_k^2\}$, see (33)[4]—it can compute the approximations in (34) if sensors report their local processes $\{\boldsymbol{D}_t^k\}_{k,t}$ to the FC, where $\boldsymbol{D}_t = \sum_{k=1}^{K} \boldsymbol{D}_t^k$. Note that each local process $\{\boldsymbol{D}_t^k\}_t$ is n-dimensional, and its entries at time t are given by

$$\left\{ d_{t,i}^k = \sum\nolimits_{p=1}^{t} \frac{\left(h_{p,i}^k\right)^2}{\sigma_k^2} \right\}_i,$$

which can be compared to (32). Hence, we propose that each sensor k sequentially report the local processes $\{\boldsymbol{D}_t^k\}_t$ and $\{\bar{V}_t^k\}_t$ to the FC, achieving linear complexity $O(n)$. On the other side, the FC, using the information received from sensors, computes the approximations $\{\tilde{\boldsymbol{D}}_t\}$ and $\{\tilde{V}_t\}$, which are then used to compute the stopping time

$$\tilde{\mathsf{T}} = \min\left\{t \in \mathbb{N} : \mathsf{Tr}\left(\tilde{\boldsymbol{U}}_t^{-1}\right) \leq \tilde{c}\right\} \tag{38}$$

and the estimator

$$\tilde{X}_{\tilde{\mathsf{T}}} = \tilde{\boldsymbol{U}}_{\tilde{\mathsf{T}}}^{-1} \tilde{V}_{\tilde{\mathsf{T}}} \tag{39}$$

similar to (31) and (30), respectively. The approximations $\mathsf{Tr}(\tilde{\boldsymbol{U}}_t^{-1})$ in (38) and $\boldsymbol{U}_{\tilde{\mathsf{T}}}$ in (39) are computed using $\tilde{\boldsymbol{D}}_t$ as in (34). The threshold $\tilde{c}$ is selected through simulations to satisfy the constraint in (24) with equality—i.e., $\mathsf{Tr}(\mathsf{Cov}(\tilde{X}_{\tilde{\mathsf{T}}} | \boldsymbol{H}_{\tilde{\mathsf{T}}})) = c$.

[4] The subscripts i and j in the set notation denote $i = 1, \ldots, n$ and $j = i, \ldots, n$. In the special case where $\mathsf{E}[(h_{t,i}^k)^2] = \mathsf{E}[(h_{t,i}^m)^2]$, $k, m, = 1, \ldots, K$, $i = 1, \ldots, n$, the correlation coefficients

$$\left\{ \xi_{ij}^k = \frac{\mathsf{E}[h_{t,i}^k h_{t,j}^k]}{\sqrt{\mathsf{E}[(h_{t,i}^k)^2] E[(h_{t,j}^k)^2]}} : i = 1, \ldots, n-1, \; j = i+1, \ldots, n \right\}_k$$

together with $\{\sigma_k^2\}$ are sufficient statistics, since, from (37), $r_{ij} = \frac{\sum_{k=1}^{K} \xi_{ij}^k / \sigma_k^2}{\sum_{k=1}^{K} 1/\sigma_k^2}$.

B. Decentralized Sequential Estimator Based on Level-Triggered Sampling

Level-triggered sampling provides a very convenient way of transmitting information in decentralized systems [19, 22]. Specifically, decentralized methods based on level-triggered sampling, transmitting low-rate information, enable highly accurate approximations and thus high-performance schemes at the FC. They significantly outperform conventional decentralized methods which sample local processes using traditional uniform sampling and send the quantized versions of samples to the FC [19, 23].

Existing methods employ level-triggered sampling to report a scalar local process to the FC. Using a similar procedure to report each distinct entry of $\bar{\boldsymbol{U}}_t^k$ and $\bar{V}_t^k$, we need $O(n^2)$ parallel procedures, which may be prohibitive in a decentralized setup for large n. Hence, we propose to use the approximations introduced in the previous subsection, achieving linear complexity $O(n)$. Moreover, for highly accurate approximations, existing methods transmit multiple bits of information per sample to overcome the overshoot problem, which again can be cumbersome even with $O(n)$ parallel procedures. To that end, we propose an alternative way to handle the overshoot problem. Particularly, in the proposed decentralized estimator, the overshoot in each sample is encoded in time by transmitting a single pulse with very short duration, which greatly helps comply with the stringent energy constraints.

We will next describe the proposed decentralized estimator based on level-triggered sampling in which each sensor nonuniformly samples the local processes $\{\mathbf{D}_t^k\}_t$ and $\{\bar{V}_t^k\}_t$ and transmits a single pulse for each sample to the FC, and the FC computes $\{\tilde{\boldsymbol{D}}_t\}$ and $\{\tilde{V}_t\}$ using received information.

1) *Sampling and Recovery of* $\boldsymbol{D}_t^k$: Each sensor k samples each entry $d_{t,i}^k$ of $\boldsymbol{D}_t^k$ at a sequence of random times $\{s_{m,i}^k\}_m$ given by

$$s_{m,i}^k \triangleq \min\left\{t \in \mathbb{N} : d_{t,i}^k - d_{s_{m-1,i}^k,i}^k \geq \Delta_i^k\right\}, \quad s_{0,i}^k = 0, \tag{40}$$

where

$$d_{t,i}^k = \sum\nolimits_{p=1}^{t} \frac{\left(h_{p,i}^k\right)^2}{\sigma_k^2},$$

$d_{0,i}^k = 0$, and $\Delta_i^k > 0$ is a constant threshold that controls the average sampling interval.[5] Note that the sampling times $\{s_{m,i}^k\}_m$ in (40) are dynamically determined by the signal to be sampled—i.e., realizations of $d_{t,i}^k$. Hence, they are random, whereas sampling times in the conventional uniform sampling are deterministic with a certain period. According to the sampling rule in (40), a sample is taken whenever the signal level $d_{t,i}^k$ increases by at least Δ_i^k since the last sampling time. Note that

$$d_{t,i}^k = \sum\nolimits_{p=1}^{t} \frac{\left(h_{p,i}^k\right)^2}{\sigma_k^2}$$

is nondecreasing in t.

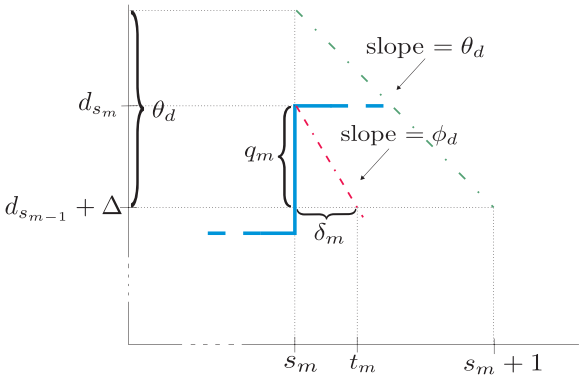

Fig. 5. Illustration of sampling time s_m, transmission time t_m, transmission delay δ_m, and overshoot q_m. We encode $q_m = (d_{s_m} - d_{s_{m-1}}) - \Delta < \theta_d$ in $\delta_m = t_m - s_m < 1$ using the slope $\phi_d > \theta_d$.

After each sampling time $s_{m,i}^k$, sensor k transmits a single pulse to the FC at time $t_{m,i}^k \triangleq s_{m,i}^k + \delta_{m,i}^k$, indicating that $d_{t,i}^k$ has increased by at least Δ_i^k since the last sampling time $s_{m-1,i}^k$. The delay $\delta_{m,i}^k$ between the transmission time and the sampling time is used to linearly encode the overshoot

$$q_{m,i}^k \triangleq \left(d_{s_{m,i}^k,i}^k - d_{s_{m-1,i}^k,i}^k\right) - \Delta_i^k \tag{41}$$

and is given by

$$\delta_{m,i}^k = \frac{q_{m,i}^k}{\phi_d} \in [0, 1), \tag{42}$$

where ϕ_d^{-1} is the slope of the linear encoding function, as shown in Fig. 5, known to sensors and the FC.

Assume a global clock—that is, the time index $t \in \mathbb{N}$ is the same for all sensors and the FC, meaning that the FC knows the potential sampling times. Assume further ultrawideband channels between sensors and the FC, in which the FC can determine the time of flight of pulses transmitted from sensors. Then the FC can measure the transmission delay $\delta_{m,i}^k$ if it is bounded by unit time—i.e., $\delta_{m,i}^k \in [0, 1)$. To ensure this, from (42) we need to have $\phi_d > q_{m,i}^k \quad \forall k, m, i$. Assuming a bound for overshoots—i.e., $q_{m,i}^k < \theta_d \quad \forall k, m, i$—we can achieve this by setting $\phi_d > \theta_d$.

Consequently, the FC can uniquely decode the overshoot by computing $q_{m,i}^k = \phi_d \delta_{m,i}^k$ (see Fig. 5), using which it can also find the increment that occurred in $d_{t,i}^k$ during the interval $(s_{m-1,i}^k, s_{m,i}^k]$ as $d_{s_{m,i}^k,i}^k - d_{s_{m-1,i}^k,i}^k = \Delta_i^k + q_{m,i}^k$ from (41). It is then possible to reach the signal level $d_{s_{m,i}^k,i}^k$ by accumulating the

[5] The subscript m in the set notation denotes $m \in \mathbb{N}$.

increments until the mth sampling time, i.e.,

$$d^k_{s^k_{m,i},i} = \sum_{\ell=1}^{m} \left(\Delta^k_i + q^k_{\ell,i}\right) = m\Delta^k_i + \sum_{\ell=1}^{m} q^k_{\ell,i}. \tag{43}$$

Using $\{d^k_{s^k_{m,i},i}\}_m$, the FC computes the staircase approximation $\tilde{d}^k_{t,i}$ as

$$\tilde{d}^k_{t,i} = d^k_{s^k_{m,i},i}, \quad t \in \left[t^k_{m,i}, t^k_{m+1,i}\right), \tag{44}$$

which is updated when a new pulse is received from sensor k and otherwise kept constant. Such approximate local signals of different sensors are next combined to obtain the approximate global signal

$$\tilde{d}_{t,i} = \sum_{k=1}^{K} \tilde{d}^k_{t,i}. \tag{45}$$

In practice, when the mth pulse in the global order regarding dimension i is received from sensor k_m at time $t_{m,i}$, instead of computing (43)–(45) the FC only updates $\tilde{d}_{t,i}$ as

$$\tilde{d}_{t_{m,i},i} = \tilde{d}_{t_{m-1,i},i} + \Delta^{k_m}_i + q_{m,i}, \tag{46}$$

$\tilde{d}_{0,i} = \epsilon$, and keeps it constant when no pulse arrives. We initialize $\tilde{d}_{t,i}$ to a small constant ϵ to prevent dividing by 0 while computing the test statistic—see (47).

Note that in general $\tilde{d}_{t_{m,i},i} \neq d_{s_{m,i},i}$, unlike (44), since all sensors do not necessarily sample and transmit at the same time. The approximations $\{\tilde{d}_{t,i}\}_i$ form $\tilde{\boldsymbol{D}}_t = \mathrm{diag}(\tilde{d}_{t,1}, \ldots, \tilde{d}_{t,n})$, which is used in (38) and (39) to compute the stopping time and estimator, respectively. Note that to determine the stopping time as in (38) we need to compute $\mathsf{Tr}(\tilde{\boldsymbol{U}}_t^{-1})$ using (34) at times $\{t_m\}$ when a pulse is received from any sensor regarding any dimension. Fortunately, when the mth pulse in the global order is received from sensor k_m at time t_m regarding dimension i_m, we can compute $\mathsf{Tr}(\tilde{\boldsymbol{U}}^{-1}_{t_m})$ recursively as follows:

$$\begin{aligned} \mathsf{Tr}\left(\tilde{\boldsymbol{U}}^{-1}_{t_m}\right) &= \mathsf{Tr}\left(\tilde{\boldsymbol{U}}^{-1}_{t_{m-1}}\right) - \frac{\kappa_{i_m}\left(\Delta^{k_m}_{i_m} + q_m\right)}{\tilde{d}_{t_m,i_m}\tilde{d}_{t_{m-1},i_m}}, \\ \mathsf{Tr}(\tilde{\boldsymbol{U}}^{-1}_0) &= \sum_{i=1}^{n} (\kappa_i/\epsilon), \end{aligned} \tag{47}$$

where κ_i is the ith diagonal element of the inverse correlation matrix $\boldsymbol{R}^{-1}$, known to the FC. In (47), pulse arrival times are assumed to be distinct for the sake of simplicity. In case multiple pulses arrive at the same time, the update rule will be similar to (47) except that it will consider all new arrivals together.

2) *Sampling and Recovery of* $\bar{V}^k_t$: Similar to (40), each sensor k samples each entry $\bar{v}^k_{t,i}$ of $\bar{V}^k_t$ at a sequence of random times $\{\alpha^k_{m,i}\}_m$ written as

$$\alpha^k_{m,i} \triangleq \min\left\{t \in \mathbb{N} : \left|\bar{v}^k_{t,i} - \bar{v}^k_{\alpha^k_{m-1,i},i}\right| \geq \gamma^k_i\right\}, \quad \alpha^k_{0,i} = 0, \tag{48}$$

where $\bar{v}^k_{t,i} = \sum_{p=1}^{t} (h^k_{p,i} y^k_p/\sigma^2_k)$ and γ^k_i is a constant threshold, available to both sensor k and the FC. It has been shown in [23, section IV-B] that $\gamma^k_i = \gamma_i$ can be determined by

$$\gamma_i \tanh\left(\frac{\gamma_i}{2}\right) = \frac{1}{R}\sum_{k=1}^{K} \left|\mathsf{E}\left[\bar{v}^k_{1,i}\right]\right| \tag{49}$$

to ensure that the FC receives messages at an average rate of R messages per unit time interval. Since $\bar{v}^k_{t,i}$ is neither increasing nor decreasing, we use two thresholds γ^k_i and $-\gamma^k_i$ in the sampling rule given in (48). Specifically, a sample is taken whenever $\bar{v}^k_{t,i}$ increases or decreases by at least γ^k_i since the last sampling time. Then, sensor k at time $p^k_{m,i} \triangleq \alpha^k_{m,i} + \beta^k_{m,i}$ transmits a single pulse $b^k_{m,i}$ to the FC, indicating whether $\bar{v}^k_{t,i}$ has changed by at least γ^k_i or $-\gamma^k_i$ since the last sampling time $\alpha^k_{m-1,i}$. We can simply write $b^k_{m,i}$ as

$$b^k_{m,i} = \mathrm{sign}\left(\bar{v}^k_{\alpha^k_{m,i},i} - \bar{v}^k_{\alpha^k_{m-1,i},i}\right), \tag{50}$$

where $b^k_{m,i} = 1$ implies that $\bar{v}^k_{\alpha^k_{m,i},i} - \bar{v}^k_{\alpha^k_{m-1,i},i} \geq \gamma^k_i$ and $b^k_{m,i} = -1$ indicates that $\bar{v}^k_{\alpha^k_{m,i},i} - \bar{v}^k_{\alpha^k_{m-1,i},i} \leq -\gamma^k_i$. The overshoot $\eta^k_{m,i} \triangleq |\bar{v}^k_{\alpha^k_{m,i},i} - \bar{v}^k_{\alpha^k_{m-1,i},i}| - \gamma^k_i$ is linearly encoded in the transmission delay as before. Similar to (42), the transmission delay is written as $\beta^k_{m,i} = \eta^k_{m,i}/\phi_v$, where ϕ_v^{-1} is the slope of the encoding function, available to sensors and the FC.

Assume again that 1) there exists a global clock among sensors and the FC, 2) the FC determines channel delay (i.e., time of flight), and 3) overshoots are bounded by a constant—i.e., $\eta^k_{m,i} < \theta_v \quad \forall k, m, i$ and we set $\phi_v > \theta_v$. With these assumptions we ensure that the FC can measure the transmission delay $\beta^k_{m,i}$ and accordingly decode the overshoot as $\eta^k_{m,i} = \phi_v \beta^k_{m,i}$. Then, upon receiving the mth pulse $b_{m,i}$ regarding dimension i from sensor k_m at time $p_{m,i}$, the FC performs the following update:

$$\tilde{v}_{p_{m,i},i} = \tilde{v}_{p_{m-1,i},i} + b_{m,i}\left(\gamma^{k_m}_i + \eta_{m,i}\right), \tag{51}$$

where $\{\tilde{v}_{t,i}\}_i$ compose the approximation $\tilde{V}_t = [\,\tilde{v}_{t,1} \cdots \tilde{v}_{t,n}\,]'$. Recall that the FC employs $\tilde{V}_t$ to compute the estimator as in (39).

The level-triggered sampling procedure at each sensor k for each dimension i is summarized in Algorithm 4. Each sensor k runs n of these procedures in parallel. The sequential estimation procedure at the FC is summarized in Algorithm 5. We assumed, for the sake of clarity, that each sensor transmits pulses to the FC for each dimension through a separate channel—i.e., parallel architecture. On the other hand, in practice the number of parallel channels can be decreased to two by using identical sampling thresholds Δ and γ for all sensors and for all dimensions in (40) and (48), respectively. Moreover, sensors can even employ a single channel to convey information about local processes $\{d^k_{t,i}\}$ and $\{\bar{v}^k_{t,i}\}$ by sending ternary digits to the FC. This is possible since pulses transmitted for $\{d^k_{t,i}\}$ are unsigned.

ALGORITHM 4 The level-triggered sampling procedure at the kth sensor for the ith dimension

1: Initialization: $t \leftarrow 0$, $m \leftarrow 0$, $\ell \leftarrow 0$, $\chi \leftarrow 0$, $\psi \leftarrow 0$
2: **while** $\chi < \Delta_i^k$ **and** $\psi \in (-\gamma_i^k, \gamma_i^k)$, **do**
3: $t \leftarrow t + 1$
4: $\chi \leftarrow \chi + \frac{(h_{t,i}^k)^2}{\sigma_k^2}$
5: $\psi \leftarrow \psi + \frac{h_{t,i}^k y_t^k}{\sigma_k^2}$
6: **end while**
7: **if** $\chi \geq \Delta_i^k$ {sample $d_{t,i}^k$} **then**
8: $m \leftarrow m + 1$
9: $s_{m,i}^k = t$
10: Send a pulse to the fusion center at time instant $t_{m,i}^k = s_{m,i}^k + \frac{\chi - \Delta_i^k}{\phi_d}$
11: $\chi \leftarrow 0$
12: **end if**
13: **if** $\psi \notin (-\gamma_i^k, \gamma_i^k)$ {sample $\bar{v}_{t,i}^k$} **then**
14: $\ell \leftarrow \ell + 1$
15: $\alpha_{\ell,i}^k = t$
16: Send $b_{\ell,i}^k = \text{sign}(\psi)$ to the fusion center at time instant $p_{\ell,i}^k = \alpha_{\ell,i}^k + \frac{|\psi| - \gamma_i^k}{\phi_v}$
17: $\psi \leftarrow 0$
18: **end if**
19: Stop if the fusion center instructs so; otherwise go to line 2

ALGORITHM 5 The sequential estimation procedure at the fusion center

1: Initialization: $\text{Tr} \leftarrow \sum_{i=1}^n \frac{\kappa_i}{\epsilon}$, $m \leftarrow 1$, $\ell \leftarrow 1$, $\tilde{d}_i \leftarrow \epsilon \ \forall i$, $\tilde{v}_i \leftarrow 0 \quad \forall i$
2: **while** $\text{Tr} < \tilde{c}$ **do**
3: Wait to receive a pulse
4: **if** mth pulse about $d_{t,i}$ arrives from sensor k at time t **then**
5: $q_m = \phi_d(t - \lfloor t \rfloor)$.
6: $\text{Tr} \leftarrow \text{Tr} - \frac{\kappa_i(\Delta_i^k + q_m)}{\tilde{d}_i(\tilde{d}_i + \Delta_i^k + q_m)}$
7: $\tilde{d}_i = \tilde{d}_i + \Delta_i^k + q_m$
8: $m \leftarrow m + 1$
9: **end if**
10: **if** ℓth pulse b_ℓ about $v_{t,j}$ arrives from sensor k at time t **then**
11: $\eta_\ell = \phi_v(t - \lfloor t \rfloor)$
12: $\tilde{v}_j = \tilde{v}_j + b_\ell(\gamma_j^k + \eta_\ell)$
13: $\ell \leftarrow \ell + 1$
14: **end if**
15: **end while**
16: Stop at time $\tilde{\mathcal{T}} = t$
17: $\tilde{\boldsymbol{D}} = \text{diag}(\tilde{d}_1, \ldots, \tilde{d}_n)$, $\tilde{\boldsymbol{U}}^{-1} = \tilde{\boldsymbol{D}}^{-1/2} \boldsymbol{R}^{-1} \tilde{\boldsymbol{D}}^{-1/2}$, $\tilde{V} = [\, \tilde{v}_1 \ \cdots \ \tilde{v}_n \,]'$
18: $\tilde{X} = \tilde{\boldsymbol{U}}^{-1} \tilde{V}$
19: Instruct sensors to stop

C. Discussions

We introduced the decentralized estimator in Section IV-B initially for a continuous-time system with infinite precision. In practice, due to bandwidth constraints, discrete-time systems with finite precision are of interest. For example, in such systems, the overshoot

$$q_{m,i}^k \in \left[j\frac{\theta_d}{N}, (j+1)\frac{\theta_d}{N} \right),$$

$j = 0, 1, \ldots, N-1$, is quantized into

$$\hat{q}_{m,i}^k = \left(j + \frac{1}{2} \right) \frac{\theta_d}{N},$$

where N is the number of quantization levels. More specifically, a pulse is transmitted at time

$$t_{m,i}^k = s_{m,i}^k + \frac{j + 1/2}{N},$$

where the transmission delay

$$\frac{j + 1/2}{N} \in (0, 1),$$

encodes $\hat{q}_{m,i}^k$. This transmission scheme is called pulse position modulation (PPM).

In ultrawideband and optical communication systems, PPM is effectively employed. In such systems, N, which denotes the precision, can be easily made large enough so that the quantization error $|\hat{q}_{m,i}^k - q_{m,i}^k|$ becomes insignificant. Compared to conventional transmission techniques which convey information by varying the power level, frequency, and/or phase of a sinusoidal wave, PPM (with ultrawideband) is extremely energy efficient at the expense of high bandwidth usage, since only a single pulse with very short duration is transmitted per sample. Hence, PPM is well suited to energy-constrained sensor network systems.

D. Simulation Results

We next provide simulation results to compare the performances of the proposed scheme with linear complexity (given in Algorithms 4 and 5), the unsimplified version of the proposed scheme with quadratic complexity, and the optimal centralized scheme. A wireless sensor network with 10 identical sensors and an FC is considered to estimate a five-dimensional deterministic vector of parameters, i.e., $n = 5$. We assume i.i.d. Gaussian noise with unit variance at all sensors, i.e., $w_t^k \sim \mathcal{N}(0, 1) \quad \forall k, t$. We set the correlation coefficients $\{r_{ij}\}$—see (37)—of the vector H_t^k to 0 in Fig. 6 and 0.5 in Fig. 7 to test the performance of the proposed scheme in the uncorrelated and correlated cases, respectively. We compare the average stopping-time performance of the proposed scheme with linear complexity to those of the other two schemes for different MSE values. In Figs. 6 and 7, the horizontal axis represents the signal-to-error ratio in dB, where nMSE $\triangleq$ MSE/$\|X\|_2^2$—i.e., the MSE normalized by the square of the Euclidean norm of the vector to be estimated.

In the uncorrelated case, where $r_{ij} = 0 \quad \forall i, j, i \neq j$, the proposed scheme with linear complexity nearly attains the performance of the unsimplified scheme with quadratic complexity, as seen in Fig. 6. This result is rather expected, since in this case $\tilde{\boldsymbol{U}}_t \cong \boldsymbol{D}_t$ for sufficiently large t, where $\tilde{\boldsymbol{U}}_t$ and $\boldsymbol{D}_t$ are used to compute the stopping time and the estimator in the unsimplified and simplified schemes, respectively. Strikingly, the decentralized

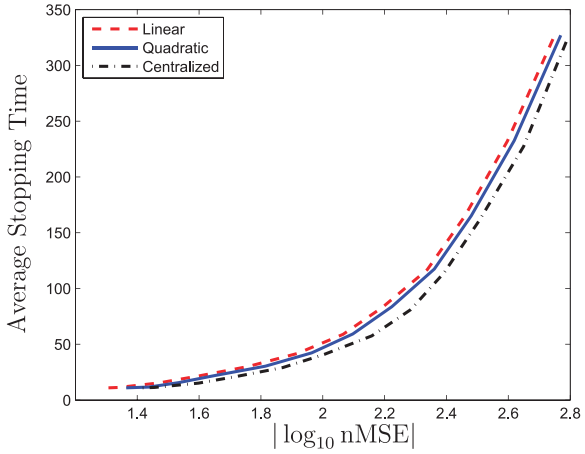

Fig. 6. Average stopping-time performances of optimal centralized scheme and decentralized schemes based on level-triggered sampling with quadratic and linear complexity versus normalized MSE values when scaling coefficients are uncorrelated, i.e., $r_{ij} = 0 \quad \forall i, j$.

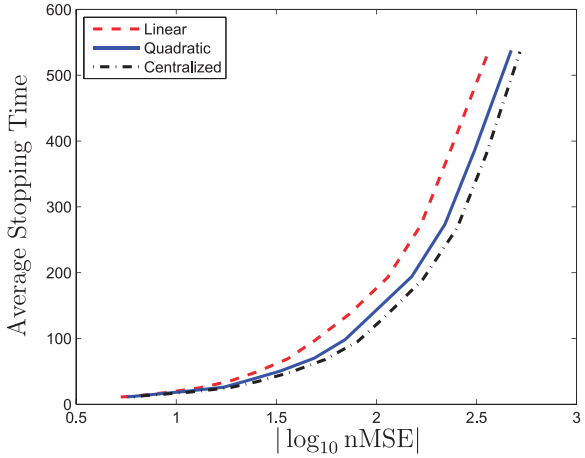

Fig. 7. Average stopping-time performances of optimal centralized scheme and decentralized schemes based on level-triggered sampling with quadratic and linear complexity versus normalized MSE values when scaling coefficients are correlated with $r_{ij} = 0.5 \quad \forall i, j$.

schemes (simplified and unsimplified) achieve very close performances to that of the optimal centralized scheme—which is obviously unattainable in a decentralized system—thanks to the efficient information transmission through level-triggered sampling. It is seen in Fig. 7 that the proposed simplified scheme exhibits an average stopping-time performance close to those of the unsimplified scheme and the optimal centralized scheme even when the scaling coefficients $\{h_{t,i}^k\}_i$ are correlated with $r_{ij} = 0.5 \quad \forall i, j, i \neq j$, justifying the simplification proposed in Section IV-A to obtain linear complexity.

In Fig. 8, we fix the normalized MSE value at 10^{-2} and plot average stopping time against the correlation coefficient r, where $r_{ij} = r \quad \forall i, j, i \neq j$. We observe an exponential growth in average stopping time of each scheme as r increases. The average stopping time of each

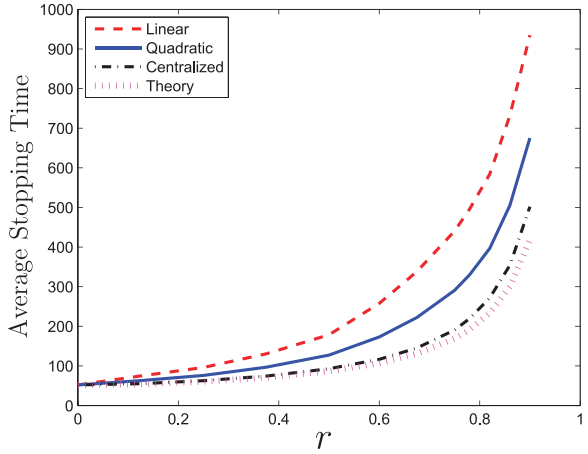

Fig. 8. Average stopping-time performances of optimal centralized scheme and decentralized schemes based on level-triggered sampling with quadratic and linear complexity versus correlation coefficient for normalized MSE fixed to 10^{-2}.

scheme becomes infinite at $r = 1$, since in this case only some multiples of a certain linear combination of the parameters to be estimated—i.e., $h_{t,1}^k \sum_{i=1}^n c_i x_i$—are observed under the noise w_t^k at each sensor k at each time t, and thus it is not possible to recover the individual parameters. Specifically, it can be shown that

$$c_i = \sqrt{\frac{\mathsf{E}\left[\left(h_{t,i}^k\right)^2\right]}{\mathsf{E}\left[\left(h_{t,1}^k\right)^2\right]}},$$

which is the same for all sensors, as we assume identical sensors. To see the mechanism that causes the exponential growth, consider the computation of $\mathsf{Tr}(\bar{\boldsymbol{U}}_t^{-1})$, which is used to determine the stopping time in the optimal centralized scheme. From (34) we write

$$\mathsf{Tr}\left(\bar{\boldsymbol{U}}_t^{-1}\right) \cong \mathsf{Tr}\left(\boldsymbol{D}_t^{-1}\boldsymbol{R}^{-1}\right) = \sum_{i=1}^{n} \frac{\kappa_i}{d_{t,i}} \tag{52}$$

for sufficiently large t, where $d_{t,i}$ and κ_i are the ith diagonal elements of the matrices $\boldsymbol{D}_t$ and $\boldsymbol{R}^{-1}$, respectively. For instance, we have $\kappa_i = 1 \quad \forall i$, $\kappa_i = 8.0435 \quad \forall i$, and $\kappa_i = \infty$, respectively, when $r = 0$, $r = 0.9$, and $r = 1$. Assuming that the scaling coefficients have the same mean and variance when $r = 0$ and $r = 0.9$, we have similar $\mathrm{d}_{t,i}$ values—see (32)—in (52), and hence the stopping time of $r = 0.9$ is approximately 8 times that of $r = 0$ for the same accuracy level. Since $\mathrm{MSE} = \mathsf{E}[\|\hat{X}_{\mathcal{T}} - X\|_2^2] = \mathsf{Tr}(\bar{\boldsymbol{U}}_{\mathcal{T}}^{-1})$ in the centralized scheme, using κ_i for different r values allows us to know approximately how the average stopping time changes as r increases for a given MSE value. As shown in Fig. 8 with the label "Theory," this theoretical curve is a good match with the numerical result. The small discrepancy at high r values is due to the high sensitivity of the WLS estimator in (30) to numerical errors when the stopping time is large. The high sensitivity is due to multiplying the matrix $\bar{\boldsymbol{U}}_{\mathcal{T}}^{-1}$ with very small entries by the vector $\bar{V}_{\mathcal{T}}$ with very large

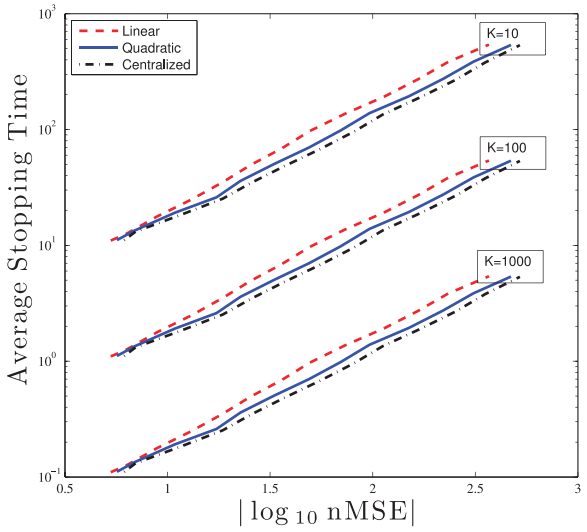

Fig. 9. Average stopping-time performances versus normalized MSE values for different sensor diversity K. Unknown parameters are correlated with $r_{ij} = 0.5 \quad \forall i, j$. Similar results are obtained for uncorrelated case.

entries while computing the estimator $\hat{X}_{\mathcal{T}}$ in (30) for a large $\mathcal{T}$. The decentralized schemes suffer from a similar high-sensitivity problem—see (39)—much more than the centralized scheme, since error is inherent in a decentralized system. Moreover, in the decentralized schemes the MSE is not given by the stopping-time statistic $\mathrm{Tr}(\tilde{\boldsymbol{U}}_t^{-1})$, and hence "Theory" does not match well the curves for the decentralized schemes. Although it cannot be used to estimate the rates of the exponential growths of the decentralized schemes, it is still useful to explain the mechanism behind them, as the decentralized schemes are derived from the centralized scheme.

To summarize, with identical sensors any estimator (centralized or decentralized) experiences an exponential growth in its average stopping time as the correlation between scaling coefficients increases, since in the extreme case of full correlation—i.e., $r = 1$—each sensor k at each time t observes a noisy sample of the linear combination

$$\sum_{i=1}^{n} x_i \sqrt{\frac{\mathsf{E}\left[\left(h_{t,i}^k\right)^2\right]}{\mathsf{E}\left[\left(h_{t,1}^k\right)^2\right]}},$$

and thus the stopping time is infinite. As a result of exponentially growing stopping time, the WLS estimator, which is the optimum estimator in our case—i.e., the minimum-variance unbiased estimator—and the decentralized estimators derived from it become highly sensitive to errors as r increases. In either uncorrelated or mildly correlated cases, which are of practical importance, the proposed decentralized scheme with linear complexity performs very close to the optimal centralized scheme, as shown in Figs. 6 and 7, respectively.

Finally, we analyze the effect of increasing number of sensors K. In Fig. 9, it is seen that the average stopping times of all schemes decay with the same rate of $1/K$, as expected for identical sensors. The small performance gaps between the centralized and decentralized schemes are preserved as K increases. Note that the decentralized algorithm proposed in Section IV-B is scalable to very large sensor networks if identical sampling thresholds are used for all sensors, in which case the FC treats the messages from all sensors in the same way.

V. CONCLUSIONS

We have considered the problem of sequential vector-parameter estimation under both centralized and decentralized settings. In the centralized setting, we have first sought the optimum sequential estimator under the classical formulation of the problem, in which expected stopping time is minimized subject to a constraint on a function of the estimator covariance. Treating the problem with optimal stopping theory, we have shown that the optimum solution is intractable for even a moderate number of parameters to be estimated. We have considered an alternative formulation that is conditional on the observed regressors, and shown that it has a simple optimum solution for any number of parameters. Using the tractable optimum sequential estimator of the conditional formulation, we have also developed a computation- and energy-efficient decentralized estimator. In the decentralized setup, to satisfy the stringent energy constraints we have proposed two novelties in the level-triggered sampling procedure, which is a nonuniform sampling technique. Finally, numerical results have demonstrated that the proposed decentralized estimator has a similar average stopping-time performance to that of the optimum centralized estimator.

APPENDIX. PROOF OF LEMMA 2

We will first prove that if $\mathcal{V}(z)$ is nondecreasing, concave, and bounded, then so is

$$G(z) = 1 + \mathsf{E}\left[\mathcal{V}\left(\frac{z}{1+zh_1^2}\right)\right].$$

That is, assume $\mathcal{V}(z)$ satisfies

1) $\frac{\mathrm{d}}{\mathrm{d}z}\mathcal{V}(z) \geq 0$,
2) $\frac{\mathrm{d}^2}{\mathrm{d}z^2}\mathcal{V}(z) < 0$, and
3) $\mathcal{V}(z) < c < \infty \quad \forall z$. Then by 3) we have

$$1 + \mathcal{V}\left(\frac{z}{1+zh_1^2}\right) < 1 + c \quad \forall z, \tag{53}$$

and thus $G(z) < 1 + c$ is bounded. Moreover,

$$\frac{\mathrm{d}}{\mathrm{d}z}\mathcal{V}\left(\frac{z}{1+zh_1^2}\right) = \frac{\frac{\mathrm{d}}{\mathrm{d}z}\mathcal{V}(z)}{\left(1+zh_1^2\right)^2} > 0 \quad \forall z \tag{54}$$

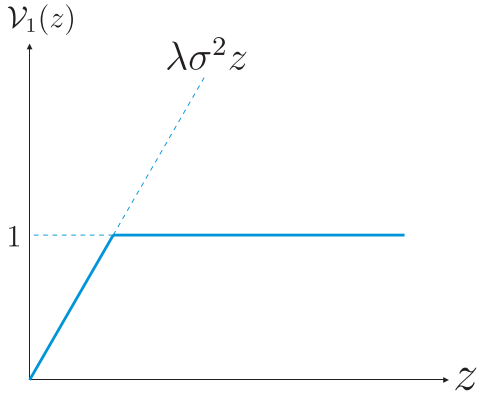

Fig. 10. Function $\mathcal{V}_1(z)$ is nondecreasing and concave.

by 1), and thus $G(z)$ is nondecreasing. Furthermore,

$$\frac{\mathrm{d}^2}{\mathrm{d}z^2}G(z) = \mathsf{E}\left[\frac{\mathrm{d}^2}{\mathrm{d}z^2}\mathcal{V}\left(\frac{z}{1+zh_1^2}\right)\right] = \mathsf{E}\left[\underbrace{\frac{\frac{\mathrm{d}^2}{\mathrm{d}z^2}\mathcal{V}(z)}{\left(1+zh_1^2\right)^4}}_{<0 \text{ by } 2)} + \underbrace{\frac{\frac{\mathrm{d}}{\mathrm{d}z}\mathcal{V}(z)}{-\left(1+zh_1^2\right)^3\Big/2h_1^2}}_{<0 \text{ by } 1) \text{ and } z=\frac{1}{u}>0}\right] \quad \forall z, \tag{55}$$

and hence $G(z)$ is concave, concluding the first part of the proof.

Now it is sufficient to show that $\mathcal{V}(z)$ is nondecreasing, concave, and bounded. Assume that the limit $\lim_{m\to\infty}\mathcal{V}_m(z) = \mathcal{V}(z)$ exists. We will prove the existence of the limit later. First, we will show that $\mathcal{V}(z)$ is nondecreasing and concave by iterating the functions $\{\mathcal{V}_m(z)\}$. Start with $\mathcal{V}_0(z) = 0$. Then

$$\mathcal{V}_1(z) = \min\left\{\lambda\sigma^2 z, 1 + \mathsf{E}\left[\mathcal{V}_0\left(\frac{z}{1+zh_1^2}\right)\right]\right\} = \min\left\{\lambda\sigma^2 z, 1\right\}, \tag{56}$$

which is nondecreasing and concave, as shown in Fig. 10. Similarly, we write

$$\mathcal{V}_2(z) = \min\left\{\lambda\sigma^2 z, 1 + \mathsf{E}\left[\mathcal{V}_1\left(\frac{z}{1+zh_1^2}\right)\right]\right\}, \tag{57}$$

where

$$1 + \mathsf{E}\left[\mathcal{V}_1\left(\frac{z}{1+zh_1^2}\right)\right]$$

is nondecreasing and concave, since $\mathcal{V}_1(z)$ is nondecreasing and concave. Hence, $\mathcal{V}_2(z)$ is nondecreasing and concave, since the point-wise minimum of a nondecreasing and concave function is again nondecreasing and concave. We can show in the same way that $\mathcal{V}_m(z)$ is nondecreasing and concave for $m > 2$—i.e., $\mathcal{V}(z) = \mathcal{V}_\infty(z)$ is nondecreasing and concave.

Next, we will show that $\mathcal{V}(z)$ is bounded. Assume that

$$\mathcal{V}(z) < \min\left\{\lambda\sigma^2 z, c\right\} = \lambda\sigma^2 z\mathbb{1}_{\{\lambda\sigma^2 z\le c\}} + c\mathbb{1}_{\{\lambda\sigma^2 z>c\}}. \tag{58}$$

Then from the definition of $\mathcal{V}(z)$ we have

$$1 + \mathsf{E}\left[\mathcal{V}\left(\frac{z}{1+zh_1^2}\right)\right] < c.$$

Since $\mathcal{V}(z)$ is nondecreasing,

$$\mathsf{E}\left[\mathcal{V}\left(\frac{z}{1+zh_1^2}\right)\right] \le \mathsf{E}\left[\mathcal{V}\left(\frac{1}{h_1^2}\right)\right].$$

From (58) we can write

$$1 + \mathsf{E}\left[\mathcal{V}\left(\frac{z}{1+zh_1^2}\right)\right] \le 1 + \mathsf{E}\left[\mathcal{V}\left(\frac{1}{h_1^2}\right)\right] < 1 + \mathsf{E}\left[\frac{\lambda\sigma^2}{h_1^2}\mathbb{1}_{\left\{\frac{\lambda\sigma^2}{h_1^2}\le c\right\}}\right] + cP\left(\frac{\lambda\sigma^2}{h_1^2} > c\right). \tag{59}$$

Recalling

$$1 + \mathsf{E}\left[\mathcal{V}\left(\frac{z}{1+zh_1^2}\right)\right] < c,$$

we want to find a c such that

$$1 + \mathsf{E}\left[\frac{\lambda\sigma^2}{h_1^2}\mathbb{1}_{\left\{\frac{\lambda\sigma^2}{h_1^2}\le c\right\}}\right] + cP\left(\frac{\lambda\sigma^2}{h_1^2} > c\right) < c. \tag{60}$$

For such a c we have

$$1 < cP\left(\frac{\lambda\sigma^2}{h_1^2} \le c\right) - \mathsf{E}\left[\frac{\lambda\sigma^2}{h_1^2}\mathbb{1}_{\left\{\frac{\lambda\sigma^2}{h_1^2}\le c\right\}}\right] = \mathsf{E}\left[\left(c - \frac{\lambda\sigma^2}{h_1^2}\right)\mathbb{1}_{\left\{\frac{\lambda\sigma^2}{h_1^2}\le c\right\}}\right] = \mathsf{E}\left[\left(c - \frac{\lambda\sigma^2}{h_1^2}\right)^+\right], \tag{61}$$

where $(\cdot)^+$ is the positive part operator. We need to show that there exists a c satisfying

$$\mathsf{E}\left[\left(c - \frac{\lambda\sigma^2}{h_1^2}\right)^+\right] > 1.$$

Note that we can write

$$\mathsf{E}\left[\left(c - \frac{\lambda\sigma^2}{h_1^2}\right)^+\right] \ge \mathsf{E}\left[\left(c - \frac{\lambda\sigma^2}{h_1^2}\right)^+\mathbb{1}_{\{h_1^2>\epsilon\}}\right] > \mathsf{E}\left[\left(c - \frac{\lambda\sigma^2}{\epsilon}\right)^+\mathbb{1}_{\{h_1^2>\epsilon\}}\right] = \left(c - \frac{\lambda\sigma^2}{\epsilon}\right)^+\mathsf{P}\left(h_1^2 > \epsilon\right), \tag{62}$$

where

$$\left(c - \frac{\lambda\sigma^2}{\epsilon}\right)^+ \to \infty$$

as $c \to \infty$, since λ and ϵ are constants. If $\mathsf{P}(h_1^2 > \epsilon) > 0$, which is always true except in the trivial case where $h_1 = 0$ deterministically, then the desired c exists.

Now what remains is to justify our initial assumption $\mathcal{V}(z) < \min\{\lambda\sigma^2 z, c\}$. We will use induction to show that the assumption holds with the c just found. From (56), we have $\mathcal{V}_1(z) = \min\{\lambda\sigma^2 z, 1\} < \min\{\lambda\sigma^2 z, c\}$, since $c > 1$. Then assume that

$$\mathcal{V}_{m-1}(z) < \min\left\{\lambda\sigma^2 z, c\right\} = \lambda\sigma^2 z \mathbb{1}_{\{\lambda\sigma^2 z \le c\}} + c\mathbb{1}_{\{\lambda\sigma^2 z > c\}}. \tag{63}$$

We need to show that $\mathcal{V}_m(z) < \min\{\lambda\sigma^2 z, c\}$, where

$$\mathcal{V}_m(z) = \min\left\{\lambda\sigma^2 z, 1 + \mathrm{E}\left[\mathcal{V}_{m-1}\left(\frac{z}{1+zh_1^2}\right)\right]\right\}.$$

Note that

$$1 + \mathrm{E}\left[\mathcal{V}_{m-1}\left(\frac{z}{1+zh_1^2}\right)\right] \le 1 + \mathrm{E}\left[\mathcal{V}_{m-1}\left(\frac{1}{h_1^2}\right)\right],$$

since $\mathcal{V}_{m-1}(z)$ is nondecreasing. Similar to (59), from (63) we have

$$\begin{aligned} 1 + \mathrm{E}\left[\mathcal{V}_{m-1}\left(\frac{1}{h_1^2}\right)\right] &< 1 + \mathrm{E}\left[\frac{\lambda\sigma^2}{h_1^2}\mathbb{1}_{\left\{\frac{\lambda\sigma^2}{h_1^2} \le c\right\}}\right] \\ &\quad + c\mathrm{P}\left(\frac{\lambda\sigma^2}{h_1^2} > c\right) < c, \end{aligned} \tag{64}$$

where the last inequality follows from (60). Hence,

$$\mathcal{V}_m(z) < \min\left\{\lambda\sigma^2 z, c\right\} \quad \forall m, \tag{65}$$

showing that $\mathcal{V}(z) < \min\{\lambda\sigma^2 z, c\}$, which is the assumption in (58).

We showed that $\mathcal{V}(z)$ is nondecreasing, concave, and bounded if it exists—i.e., the limit $\lim_{m\to\infty}\mathcal{V}_m(z)$ exists. Note that we showed in (65) that the sequence $\{\mathcal{V}_m\}$ is bounded. If we also show that $\{\mathcal{V}_m\}$ is monotonic—e.g., nondecreasing—then it converges to a finite limit $\mathcal{V}(z)$. We will again use induction to show the monotonicity of $\{\mathcal{V}_m\}$. From (56) we write $\mathcal{V}_1(z) = \min\{\lambda\sigma^2 z, 1\} \ge \mathcal{V}_0(z) = 0$. Assuming $\mathcal{V}_{m-1}(z) \ge \mathcal{V}_{m-2}(z)$, we need to show that $\mathcal{V}_m(z) \ge \mathcal{V}_{m-1}(z)$. Using their definitions, we write

$$\mathcal{V}_m(z) = \min\left\{\lambda\sigma^2 z, 1 + \mathrm{E}\left[\mathcal{V}_{m-1}\left(\frac{z}{1+zh_1^2}\right)\right]\right\}$$

and

$$\mathcal{V}_{m-1}(z) = \min\left\{\lambda\sigma^2 z, 1 + \mathrm{E}\left[\mathcal{V}_{m-2}\left(\frac{z}{1+zh_1^2}\right)\right]\right\}.$$

We have

$$1 + \mathrm{E}\left[\mathcal{V}_{m-1}\left(\frac{z}{1+zh_1^2}\right)\right] \ge 1 + \mathrm{E}\left[\mathcal{V}_{m-2}\left(\frac{z}{1+zh_1^2}\right)\right]$$

due to the assumption $\mathcal{V}_{m-1}(z) \ge \mathcal{V}_{m-2}(z)$, and hence $\mathcal{V}_m(z) \ge \mathcal{V}_{m-1}(z)$.

To conclude, we proved that $\mathcal{V}_m(z)$ is nondecreasing and bounded in m, and thus the limit $\mathcal{V}(z)$ exists, which was also shown to be nondecreasing, concave, and bounded. Hence, $G(z)$ is nondecreasing, concave, and bounded.

REFERENCES

[1] Akyildiz, I. F., Su, W., Sankarasubramaniam, Y., and Cayirci, E.
A survey on sensor networks.
IEEE Communications Magazine, **40**, 8 (Aug. 2002), 102–114.

[2] Das, A. K., and Mesbahi, M.
Distributed linear parameter estimation over wireless sensor networks.
IEEE Transactions on Aerospace and Electronic Systems, **45**, 4 (Oct. 2009), 1293–1306.

[3] Fang, J., and Li, H.
Adaptive distributed estimation of signal power from one-bit quantized data.
IEEE Transactions on Aerospace and Electronic Systems, **46**, 4 (Oct. 2010), 1893–1905.

[4] Ribeiro, A., and Giannakis, G. B.
Bandwidth-constrained distributed estimation for wireless sensor networks—Part II: Unknown probability density function.
IEEE Transactions on Signal Processing, **54**, 7 (July 2006), 2784–2796.

[5] Msechu, E. J., and Giannakis, G. B.
Sensor-centric data reduction for estimation with WSNs via censoring and quantization.
IEEE Transactions on Signal Processing, **60**, 1 (Jan. 2012), 400–414.

[6] Xiao, J.-J., Cui, S., Luo, Z.-Q., and Goldsmith, A. J.
Linear coherent decentralized estimation.
IEEE Transactions on Signal Processing, **56**, 2 (Feb. 2008), 757–770.

[7] Luo, Z.-Q., Giannakis, G. B., and Zhang, S.
Optimal linear decentralized estimation in a bandwidth constrained sensor network.
In *International Symposium on Information Theory*, Adelaide, Australia, Sept. 2005, 1441–1445.

[8] Schizas, I. D., Giannakis, G. B., and Luo, Z.-Q.
Distributed estimation using reduced-dimensionality sensor observations.
IEEE Transactions on Signal Processing, **55**, 8 (Aug. 2007), 4284–4299.

[9] Schizas, I. D., Ribeiro, A., and Giannakis, G. B.
Consensus in ad hoc WSNs with noisy links—Part I: Distributed estimation of deterministic signals.
IEEE Transactions on Signal Processing, **56**, 1 (Jan. 2008), 350–364.

[10] Stankovic, S. S., Stankovic, M. S., and Stipanovic, D. M.
Decentralized parameter estimation by consensus based stochastic approximation.
IEEE Transactions on Automatic Control, **56**, 3 (Mar. 2011), 531–543.

[11] Zhao, T., and Nehorai, A.
Distributed sequential Bayesian estimation of a diffusive source in wireless sensor networks.
IEEE Transactions on Signal Processing, **55**, 4 (Apr. 2007), 1511–1524.

[12] Borkar, V., and Varaiya, P. P.
Asymptotic agreement in distributed estimation.
IEEE Transactions on Automatic Control, **27**, 3 (June 1982), 650–655.

[13] Xiao, J.-J., Ribeiro, A., Luo, Z.-Q., and Giannakis, G. B.
Distributed compression-estimation using wireless sensor networks.
IEEE Signal Processing Magazine, **23**, 4 (July 2006), 27–41.

[14] Ghosh, M., Mukhopadhyay, N., and Sen, P. K.
Sequential Estimation. New York: Wiley, 1997.

[15] Braca, P., Marano, S., Matta, V., and Willett, P.

Asymptotic optimality of running consensus in testing binary hypotheses.
IEEE Transactions on Signal Processing, **58**, 2 (Feb. 2010), 814–825.

[16] Bajovic, D., Jakovetic, D., Xavier, J., Sinopoli, B., and Moura, J. M. F.
Distributed detection via Gaussian running consensus: Large deviations asymptotic analysis.
IEEE Transactions on Signal Processing, **59**, 9 (Sept. 2011), 4381–4396.

[17] Cattivelli, F. S., and Sayed, A. H.
Distributed detection over adaptive networks using diffusion adaptation.
IEEE Transactions on Signal Processing, **59**, 5 (May 2011), 1917–1932.

[18] Fellouris, G.
Asymptotically optimal parameter estimation under communication constraints.
The Annals of Statistics, **40**, 4 (2012), 2239–2265.

[19] Yılmaz, Y., and Wang, X.
Sequential decentralized parameter estimation under randomly observed Fisher information.
IEEE Transactions on Information Theory, **60**, 2 (Feb. 2014), 1281–1300.

[20] Veeravalli, V. V., Basar, T., and Poor, H. V.
Decentralized sequential detection with a fusion center performing the sequential test.
IEEE Transactions on Information Theory, **39**, 2 (Mar. 1993), 433–442.

[21] Hussain, A. M.
Multisensor distributed sequential detection.
IEEE Transactions on Aerospace and Electronic Systems, **30**, 3 (July 1994), 698–708.

[22] Fellouris, G., and Moustakides, G. V.
Decentralized sequential hypothesis testing using asynchronous communication.
IEEE Transactions on Information Theory, **57**, 1 (Jan. 2011), 534–548.

[23] Yılmaz, Y., Moustakides, G. V., and Wang, X.
Cooperative sequential spectrum sensing based on level-triggered sampling.
IEEE Transactions on Signal Processing, **60**, 9 (Sept. 2012), 4509–4524.

[24] Yılmaz, Y., Moustakides, G. V., and Wang, X.
Channel-aware decentralized detection via level-triggered sampling.
IEEE Transactions on Signal Processing, **61**, 2 (Jan. 2013), 300–315.

[25] Yılmaz, Y., and Wang, X.
Sequential distributed detection in energy-constrained wireless sensor networks.
IEEE Transactions on Signal Processing, **62**, 12 (June 2014), 3180–3193.

[26] Braca, P., Marano, S., Matta, V., and Willett, P.
Consensus-based Page's test in sensor networks.
Signal Processing, **91**, 4 (2011), 919–930.

[27] Ghosh, B. K.
On the attainment of the Cramér–Rao bound in the sequential case.
Sequential Analysis: Design Methods and Applications, **6**, 3 (1987), 267–288.

[28] Grambsch, P.
Sequential sampling based on the observed Fisher information to guarantee the accuracy of the maximum likelihood estimator.
The Annals of Statistics, **11**, 1 (1983), 68–77.

[29] Guerriero, M., Pozdnyakov, V., Glaz, J., and Willett, P.
A repeated significance test with applications to sequential detection in sensor networks.
IEEE Transactions on Signal Processing, **58**, 7 (July 2010), 3426–3435.

[30] Shiryaev, A. N.
Optimal Stopping Rules, Berlin: Springer, 2008.

[31] Efron, B., and Hinkley, D. V.
Assessing the accuracy of the maximum likelihood estimator: Observed versus expected Fisher information.
Biometrika, **65**, 3 (1978), 457–483.

[32] Vercauteren, T., and Wang, X.
Decentralized sigma-point information filters for target tracking in collaborative sensor networks.
IEEE Transactions on Signal Processing, **53**, 8 (Aug. 2005), 2997–3009.

Yasin Yılmaz (S'11—M'14) received B.Sc., M.Sc., and Ph.D. degrees in electrical engineering from, respectively, Middle East Technical University, Ankara, Turkey, in 2008; Koc University, Istanbul, Turkey, in 2010; and Columbia University, New York, in 2014. He is currently a postdoctoral research fellow at the University of Michigan, Ann Arbor. His research interests include machine learning, big data analytics, multimodal data fusion, statistical signal processing, cyber-physical systems, event-triggered systems, and sequential analysis.

George V. Moustakides (M'82—SM'97) was born in Drama, Greece, in 1955. He received a diploma in electrical and mechanical engineering from the National Technical University of Athens, Greece, in 1979; an M.Sc. degree in systems engineering from the Moore School of Electrical Engineering, University of Pennsylvania, Philadelphia, in 1980; and a Ph.D. degree in electrical engineering and computer science from Princeton University, Princeton, New Jersey, in 1983. Since 2007 he has been a professor with the department of electrical and computer engineering, University of Patras, Patras, Greece. Prof. Moustakides has also held several appointments as visiting scholar, senior researcher, and adjunct professor at Princeton University, the University of Pennsylvania, Columbia University, the University of Maryland, the Georgia Institute of Technology, the University of Southern California, and INRIA. His interests include sequential detection, statistical signal processing, and signal processing for hearing aids.

Xiaodong Wang (S'98—M'98—SM'04—F'08) received a Ph.D. degree in electrical engineering from Princeton University. He is a professor of electrical engineering at Columbia University in New York. Dr. Wang's research interests fall in the general areas of computing, signal processing, and communications, and he has published extensively in these areas. Among his publications is a book entitled *Wireless Communication Systems: Advanced Techniques for Signal Reception*, published by Prentice Hall in 2003. His current research interests include wireless communications, statistical signal processing, and genomic signal processing. Dr. Wang received the 1999 NSF CAREER Award, the 2001 IEEE Communications Society and Information Theory Society Joint Paper Award, and the 2011 IEEE Communication Society Award for Outstanding Paper on New Communication Topics. He has served as an Associate Editor for *IEEE Transactions on Communications*, *IEEE Transactions on Wireless Communications*, *IEEE Transactions on Signal Processing*, and *IEEE Transactions on Information Theory*. He is a Fellow of the IEEE and listed as an ISI highly-cited author.